

Chapter Nine

WATER CHEMISTRY

Due to the imbalance between excessive groundwater exploitation and limited natural recharge, a significant depletion of groundwater has occurred in most aquifers of UAE. In fact, the water resources in the UAE have been over exploited to meet the increasing water demand, especially for domestic and agricultural purposes, during the last four decades. Over-pumping practices has resulted into depletion of groundwater resources, severe salt-water intrusion and degradation of groundwater quality. Evidences indicated that groundwater levels have declined sharply in many farming and urban areas. To minimize this impact, the UAE government has constructed more than 114 detention and retention dams and barriers within and across the outlets of major wadis. In addition, several observation wells were installed to monitor the groundwater levels, as well as to detect changes of the groundwater quality. Detention dams are designed to control the flow velocities and to allow appropriate time for the groundwater recharge process to take place. While, retention dams are designed to store large quantities of surface water and to raise the hydraulic heads in shallow aquifer systems. The stored water can be used directly for irrigation and domestic purposes.

9.1 Surface Water Chemistry

In this section, hydrochemical and isotopic data (^{18}O , ^2H and ^3H) were used to study recharge mechanism and effectiveness of Wurayah dam in recharging the shallow aquifer systems within the study area.

The Wurayah dam was built in 1997, and is located approximately 5 km northwest the city of Khor Fakkan (ENTEC, 1996). This dam was constructed on fractured Semail Ophiolite bedrock, which comprises mineralized assemblages of serpentinite and gabbroic rocks. The catchment area of the Wurayah Basin is 129 km².

Several sampling periods were undertaken in the study areas during the period of December 2002-June 2003. Figure 9.1 shows the location map of the sampling sites in the studied areas. Water samples were generally collected in rinsed plastic bottles, and

analyzed for major cations (Ca^{2+} , Mg^{2+} , Na^+ and K^+) and anions (HCO_3^- , CO_3^{2-} , Cl^- , SO_4^{2-} and NO_3^-) in the Ministry of Environment and Water (MEW) laboratories in the UAE. Determination of stable isotopes ($\delta^{18}\text{O}$ and $\delta^2\text{H}$) values were performed in Syria by means of a Finnigan Mat DELTA^{Plus} mass spectrometer. The tritium determinations were also performed (after electrolysis) in Syria, by using a liquid scintillation counter (Quantulus 1220). Measurement accuracy for $\delta^{18}\text{O}$ and $\delta^2\text{H}$ and ^3H were ± 0.1 , ± 1.0 ‰, and ± 1 tritium unit (TU), respectively (Seif, 2010).

The major ion concentrations and total dissolved solids (TDS) of water samples collected from the Wurayah Basin wells are listed in Table 9.1. The mean TDS value of surface water in the dam reservoir was 119 milligrams per litre (mg/l). The chemistry of water samples collected from wells tapping the shallow aquifer at longer distances from the dam site (Wur5) are characterized by high TDS values, whereas those located near the dam (Wur3) are characterized by low TDS values, indicating a possible recharge from the dam reservoir. This hypothesis is confirmed by the Schoeller-Berkalof diagram (Figure 9.1), which shows similar water chemistry of reservoir water and groundwater collected from observation wells. However, the slight difference in Ca^{2+} and Mg^{2+} concentrations between the reservoir (surface water) and the observation wells (groundwater) can be explained by a cation exchange with the clay minerals present in the shallow aquifer.

Table 9.1 Results of chemical analysis of water samples collected from the Wurayah dam reservoir and the surrounding observation wells. Concentrations are in mg/l (Almatari, 2010).

Site code	Ca^{2+}	Mg^{2+}	Na^+	K^+	CO_3^{2-}	HCO_3^-	Cl^-	SO_4^{2-}	NO_3^-	TDS
Wur3	6.2	40.1	23.4	2.0	6.0	109.3	48.3	23.2	6.8	257.4
Wur5	3.5	32.0	25.5	3.5	4.5	83.5	65.5	65.5	29.0	258.5
Wur6	3.7	21.1	49.9	6.2	7.4	92.0	72.3	19.5	3.2	278.5
Wur Dam	16.8	8.7	6.3	1.8	0.0	62.5	21.4	6.6	6.8	119.0

The Piper diagram (Figure 9.2) supports also this hypothesis, and shows the similarity of water types in the reservoir and observation wells, especially those of Wur3 and Wur5. The relationship between Cl^- and Na^+ shows that the water samples of observation wells fit the same line of surface water samples from the Wurayah dam reservoir (Figure 9.3).

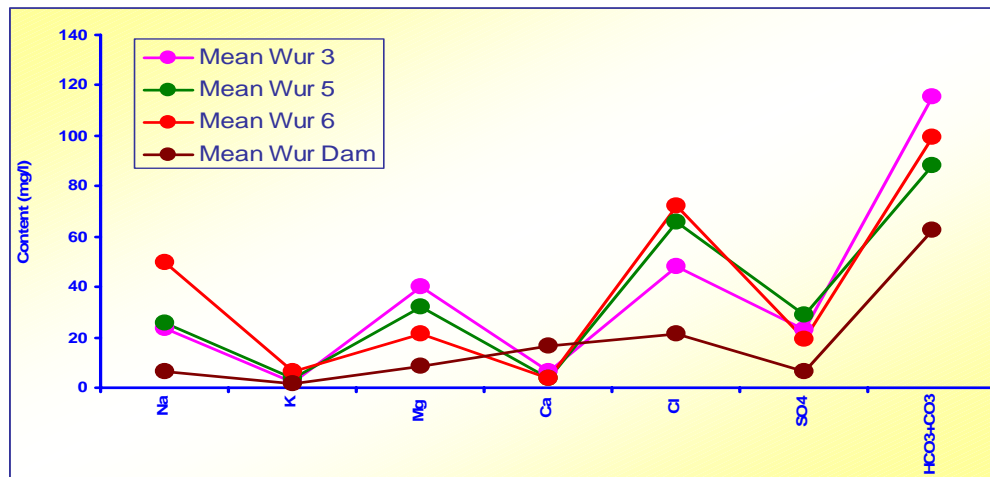


Figure 9.1 Schoeller-Berkalof diagram of the mean chemical composition of surface water and groundwater samples collected from Wadi Wurayah Basin (Almatari, 2010).

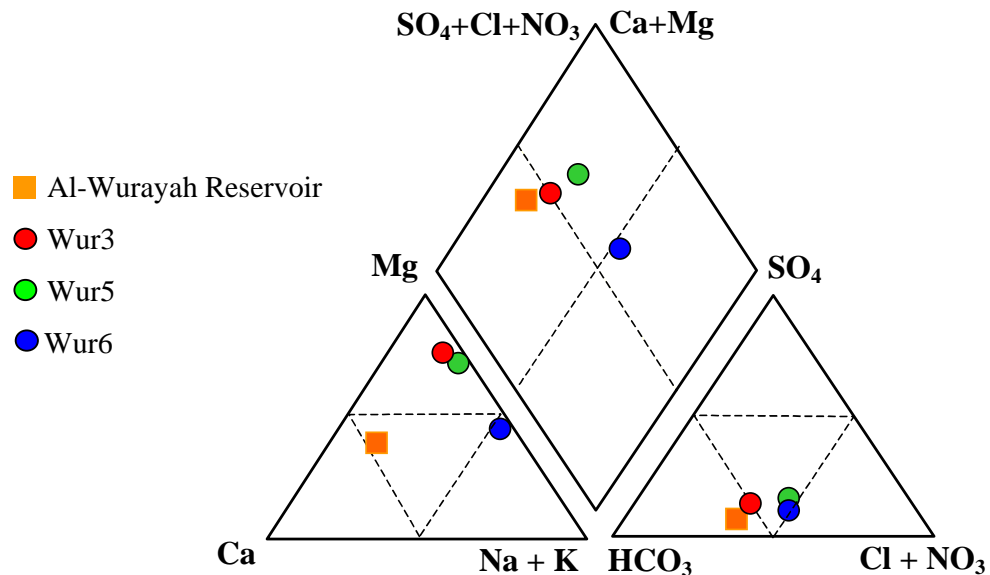


Figure 9.2 Piper diagram of the mean chemical composition of surface water and groundwater samples collected from Wadi Wurayah Basin (Almatari, 2010).

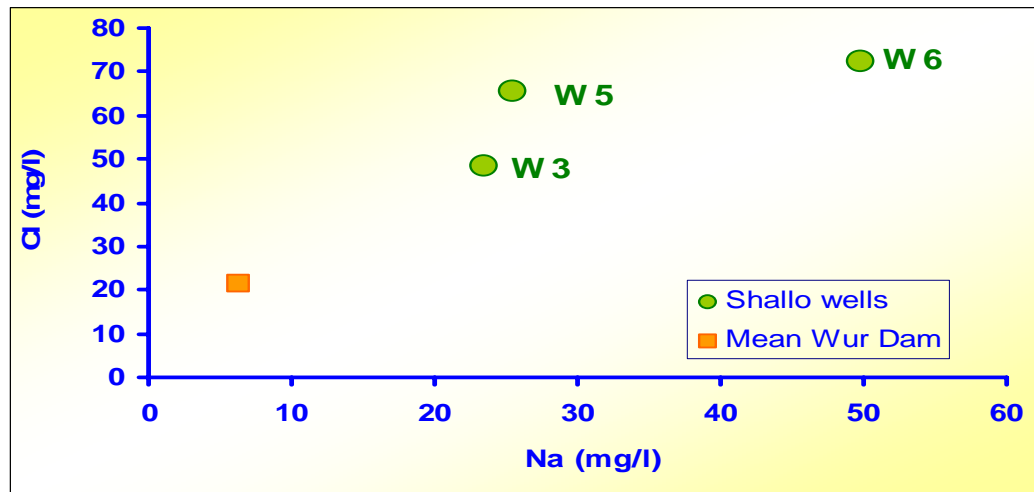


Figure 9.3 Graph illustrating the relationship between mean Cl^- and Na^+ concentrations of surface water and groundwater samples collected from Wadi Wurayah Basin (Almatari, 2010).

The position of each groundwater sample along this mixing line is proportional to the distance from the dam site, indicating a possible mixing with water having a similar origin to that in the dam reservoir.

9.2 Isotope Hydrology

The available isotopic data of rainfall was used to define the local meteoric water line (LMWL). This line was estimated on a basis of mean isotopic data obtained within another work, realized by Kulkarni et al. (1998) between 1984 and 1990 in the UAE. Accordingly, the isotopic rainfall data reveals the existence of the following features (Figure 9.4):

- The ^2H - ^{18}O diagram shows that about 80% of samples fall between the global meteoric water line (GMWL), defined by a deuterium excess (d) rounded 10‰ (Craig, 1961), and the eastern Mediterranean meteoric water line (EMWL), defined by a deuterium excess (d) value of the order of 22‰ (Nir, 1967; Geyh, 2000; Geyh, 2001). The rest of samples reflect the evaporation effect, especially the rain samples collected during winter months.

- By considering only the non-evaporated water, mostly responsible for the recharge of the shallow aquifer, the sample representative points fit clearly a line close to that of the eastern Mediterranean meteoric water. This line ($^2\text{H}=8^{18}\text{O}+17$) reveals that a significant air masses are coming from the northwest, and most probably crossing over the Mediterranean region.

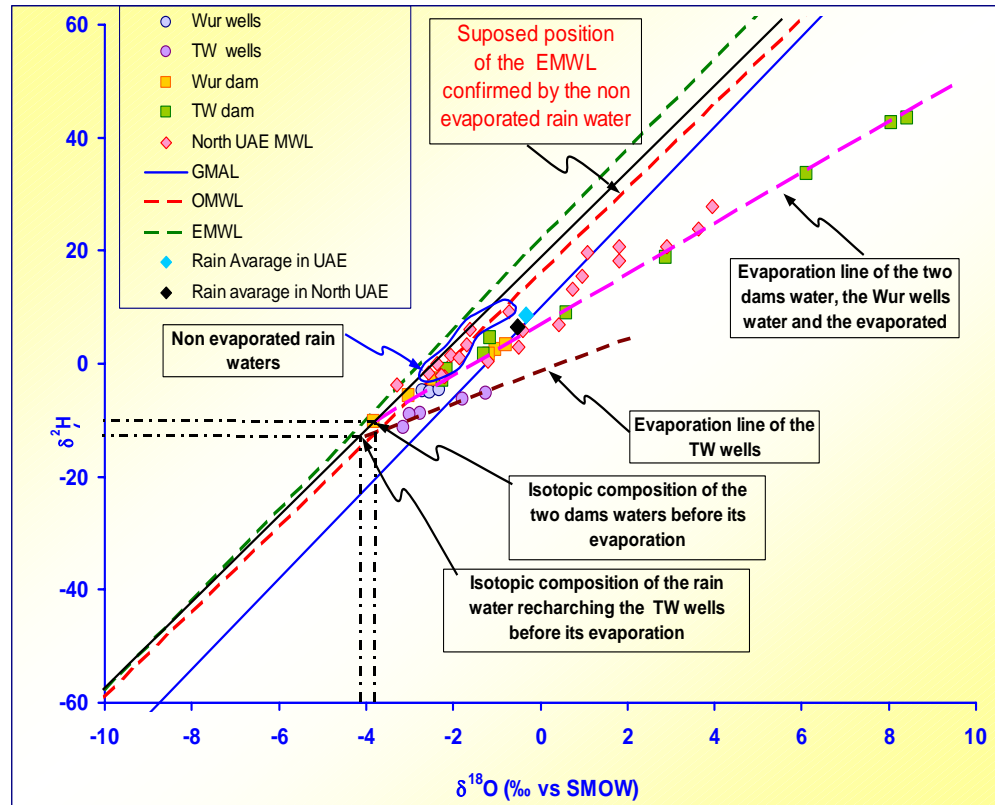


Figure 9.4 The ^2H - ^{18}O relationships of rainfall and shallow groundwater samples collected from wadi Wurayah Basin (Almatari, 2010).

- This local meteoric water line is in a good agreement with that of north Oman ($^2\text{H}=8^{18}\text{O}+16$), defined by Dansgaard (1964) on a basis of rainfall data of significant precipitation amounts (>20 mm), allowing the saturation of air column and minimizing the evaporation from of rainfall droplets.

During this study, the available isotopic data of rainfall samples have been used to define the mean stable isotopes (^{18}O , ^2H) concentrations of water samples collected

from the observation wells and Wurayah dam reservoir during the period December 2002-June 2003 (Table 9.2). The Wells Wur3 and Wur6 were sampled 14 times, while the Well Wur5 and Wurayah Reservoir were sampled 6 times.

Table 9.2 Minimum, maximum and average values of stable isotopes (^{18}O and ^2H) of water samples collected from Wadi Wurayah Basin (Almatari, 2010).

Site code	Minimum		Maximum		Average	
	$\delta^2\text{H}$ (‰)	$\delta^{18}\text{O}$ (‰)	$\delta^2\text{H}$ (‰)	$\delta^{18}\text{O}$ (‰)	$\delta^2\text{H}$ (‰)	$\delta^{18}\text{O}$ (‰)
Wur3	- 5.90	- 2.86	- 3.60	- 2.58	- 4.81	- 2.71
Wur5	-2.86	- 2.82	- 2.54	- 2.54	- 5.05	- 2.53
Wur6	- 2.82	- 2.38	- 3.32	- 2.22	- 4.54	- 2.32
Wur Dam	- 3.83	- 3.30	- 3.30	- 0.78	- 1.83	- 2.04

The maximum and average values of stable isotope concentrations of the groundwater in the observation wells are represented in the $^2\text{H}/^{18}\text{O}$ diagram (Figure 9.4). The concentration of oxygen-18 and deuterium in the dam reservoir (surface water) and rainwater samples, collected between 1984-1990 from the northern and eastern UAE are shown in Figure 9.4. Stable isotopes data of Wadi Wurayah Basin (Figure 9.4; Table 9.2), shows that there is a clear similarity between the trend of evaporated samples of precipitation and the surface water sample collected from the dam reservoir. This trend completely coincides with the groundwater evaporation line of the observation wells, indicating that this water has the same origin, and thus, the groundwater in the observation wells may mostly be recharged from the dam reservoir water.

In order to calculate the contribution of recharge coming from the dam reservoir water towards the shallow aquifer in Wadi Wurayah Basin, an isotopic mass balance, using the stable isotopes data and their relationships, was applied. Table 9.3 shows that the contribution dam reservoir water to aquifer recharge varies between 22% and 43%.

The result of this isotopic mass balance showed that groundwater in the observation wells represents a mixture of the dam reservoir water and the present-day rains. The computed values indicate the importance of the dam reservoir water in recharging the

observation wells tapping the shallow aquifer, especially Wells Wur3 and Wur5, which are very close to the dam site (Figure 9.1).

Table 9.3 Percentage (%) Contribution Wurayah dam reservoir to aquifer recharge, using isotopic mass balance (Almatari, 2010).

Site code	Average $\delta^{18}\text{O}$ (‰, V-SMOW)	Dam reservoir contribution to aquifer recharge (%)
Wur3	-2.71	43.02
Wur5	-2.53	34.1
Wur6	-2.32	22.09

9.3 Groundwater Chemistry

To study the hydrogeochemical parameters of the groundwater in the area of the study, two rounds of sampling were made in 2005 and 2009. In 2005, sixteen (16) groundwater samples were collected from water wells tapping the eastern gravel aquifer (Figure 9.5; Tables 9.4 and 9.5).

Table 9.4 Information of water wells sampled for the present study during 2005 and 2009. Well locations are shown in Figure 9.5 (ALHOGARATY).

Ser. No.	Well No.	Well code and location	Sampling Date	Northing	Easting
1	2	PNT - 2 (Dadinah - Fuj)	02.04.05	2820142.00	435578.00
2	3	PNT - 3 (Dadinah - Fuj)	02.04.05	2820195.00	435616.00
3	4	PNT - 4 (Dadinah - Fuj)	02.04.05	2820161.00	436630.00
4	5	PNT - 5 (Dadinah - Fuj)	02.04.05	2820013.00	435309.00
5	6	WUR - 1 (W. Wurayah)	07.05.05	2809291.32	427192.92
6	7	WUR - 2 (W. Wurayah)	07.05.05	2807961.45	429200.62
7	8	WUR - 3 (W. Wurayah)	07.05.05	2807160.87	430234.51
8	9	WUR - 4 (W. Wurayah)	07.05.05	2808298.10	431006.83
9	10	WUR - 5 (W. Wurayah)	07.05.05	2809560.39	431797.95
10	11	WUR - 6 (W. Wurayah)	07.05.05	2811023.81	434154.23
11	12	WUR - 7 (W. Wurayah)	07.05.05	2811139.59	435021.21
12	13	ZKT - 1 (W. Zikt)	07.05.05	2821627.68	429810.71
13	14	ZKT - 2 (W. Zikt)	07.05.05	2822890.72	430736.07
14	15	ZKT - 3 (W. Zikt)	07.05.05	2822517.23	434024.65
15	16	ZKT - 4 (W. Zikt)	07.05.05	2822917.59	431261.30
16	17	ZKT - 5 (W. Zikt)	07.05.05	2823637.24	434166.26

In 2009, sixteen (16) groundwater samples were from the same wells tapping the same aquifer in order to monitor possible changes in groundwater chemistry and

quality. The samples were chemically analyzed for major cations and anions and the results are listed in Table 9.6. The obtained results are discussed in the following, in term of the regional hydrogeochemical properties and horizontal zonation of the groundwater.

Table 9.5 Results of chemical analysis of groundwater samples collected from the eastern gravel aquifer in 2005. Concentrations are in milligrams per liter (mg/l) (ALHOGARATY).

No.	pH	TDS	TH	Ca	Mg	Na	K	HCO ₃	SO ₄	Cl	SAR
1	7.4	8512	476	134	342	1700	53	509	934	2918	17.71
2	7.7	4720	243	62	181	900	140	286	589	1529	13.05
3	7.2	11872	927	275	652	2100	65	361	1708	4213	15.73
4	7.2	11408	836	262	574	2050	53	338	1416	4103	16.23
5	7.9	326	49	8	41	25	2	195	50	89	0.8
6	8.1	294	42	8	34	27	2	159	44	71	0.95
7	8.4	237	37	7	30	19	1	146	39	53	0.7
8	8.3	269	39	6	33	22	1	159	39	64	0.8
9	8.3	269	34	3	31	26	3	134	50	78	0.9
10	8.5	243	21	4	17	45	3	122	37	78	2.2
11	8.0	678	109	32	77	56	3	214	153	270	1.2
12	7.8	211	36	9	27	16	1	134	29	53	0.6
13	8.0	230	34	4	30	19	1	134	37	71	0.6
14	7.9	250	35	2	33	21	1	110	38	71	0.8
15	8.1	230	34	3	31	20	1	122	38	71	0.8
16	8.0	256	31	2	29	27	2	122	38	82	1.1

Table 9.6 Results of chemical analysis of groundwater samples collected from the eastern gravel aquifer in 2009. Concentrations are in milligrams per liter (mg/l) (ALHOGARATY).

No.	pH	TDS	TH	Ca	Mg	Na	K	HCO ₃	SO ₄	Cl	SAR
1	7.1	6680	484	144	340	1670	52	501	965	2987	17.7
2	7.6	3776	261	65	196	1000	154	289	507	1543	13.1
3	7.3	5700	933	278	655	2200	76	350	1688	421	15.7
4	7.9	8835	830	254	576	2088	59	329	1399	4100	16.2
5	7.8	513	59	8	51	34	23	232	76	89	0.7
6	7.5	507	199	167	32	32	2	145	42	87	1
7	8.0	300	39	7	32	22	1.5	152	34	51	0.6
8	7.9	339	37	6	31	20	1	154	44	83	7.8
9	7.5	428	54	22	32	45	66	136	49	78	1
10	8.0	354	52	21	31	45	2.5	130	48	76	2
11	8.0	891	121	45	76	55	2	240	165	276	1
12	7.0	330	46	23	23	33	3	145	37	66	0.7
13	7.6	321	37	6	31	22	2	143	41	76	0.7
14	7.8	309	40	4	36	27	2	123	42	75	0.6
15	7.5	319	42	5	37	29	1.5	128	41	77	7.5
16	8.0	343	36	3	33	36	2.5	126	45	97	1.2

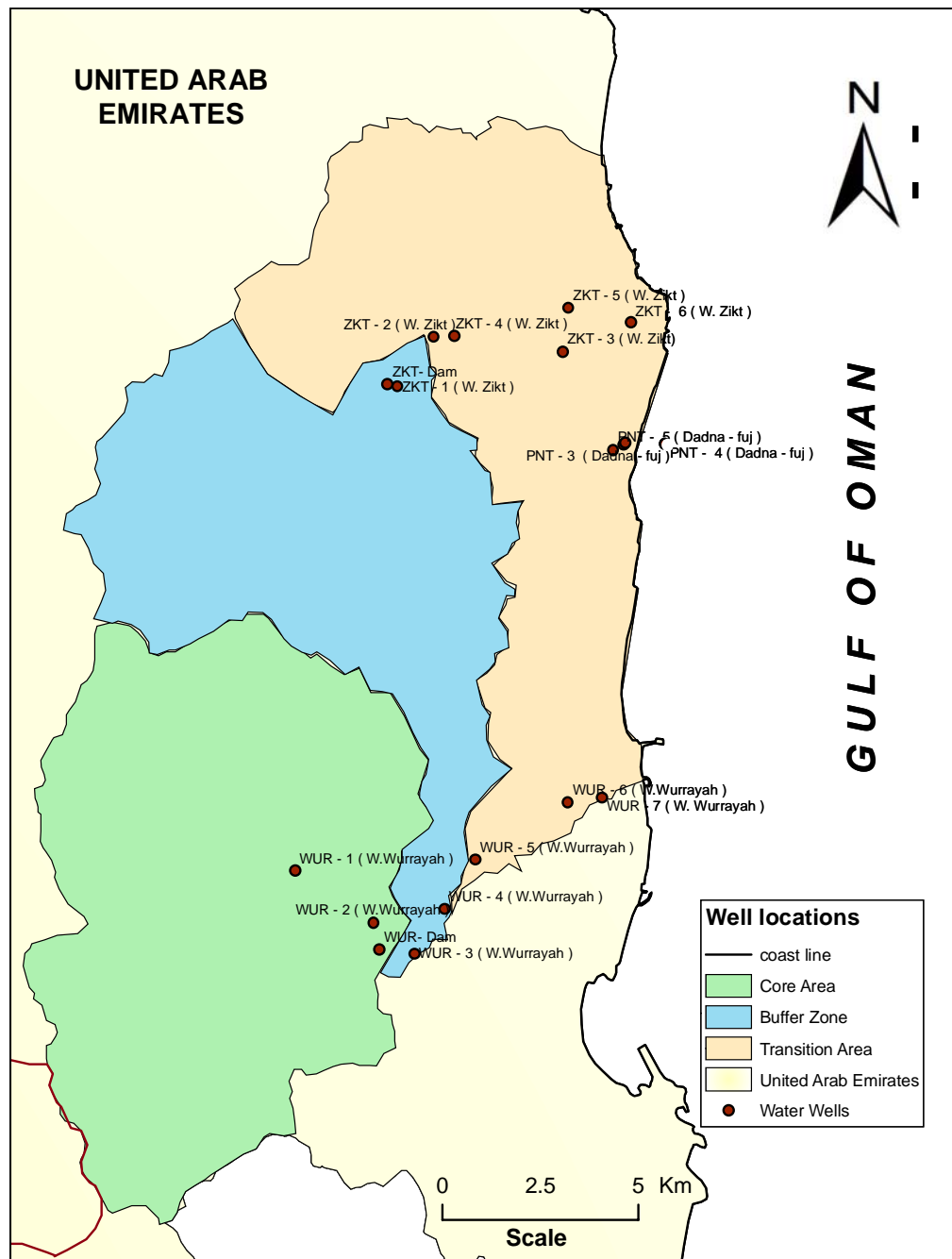


Figure 9.5 Locations of water wells sampled for chemical analysis of groundwater in the eastern gravel aquifer within the study area (ALHOGARATY).

9.3.1 Total Dissolved Solids

The total dissolved solids (TDS) in a water sample are a measure of all solid materials in solution whether ionized or not. It does not include suspended sediments, colloids or dissolved gases. The TDS content in groundwater is an indication of its salinity. The groundwater salinity within the study area reaches its lowest values near water divide line, in the western side of the study area, and increases to the east in the direction of groundwater flow (Figures 9.6 and 9.7). The high groundwater salinity at the outlets of main wadis near the Rul Dibba and Dadinah villages is due to excessive groundwater pumping for all purposes. Groundwater in the study area varies from fresh water (TDS ranging from 500 to <1,000 mg/l near the water divide line; Table 9.7) to brackish water in the eastern and northeastern parts of the study area (TDS ranging from >1,000 to 10,000 mg/l). Saline water (TDS >10,000) occurs in the outlet area of main wadis, near the Gulf of Oman coast (Figures 9.6 and 9.7).

Table 9.7 Classification of the groundwater types based on total concentration of dissolved solids (Fetter, 2001).

Water Type	Total Dissolved Solids (mg/l)
Fresh water	0 - 1,000
Brackish water	1,000 - 10,000
Saline water	10,000 - 100,000
Brine	> 100,000

Isosalinity contour maps (Figures 9.8 and 9.9) of groundwater samples collected from Wadi Wurayah area during 2005 and 2009 indicate that the groundwater salinity increases from the west to east, in the direction of groundwater flow. The 1000 mg/l contour moved further west in 2009 compared with 2005.

This high salinity is probably due to the intensive pumping activities in this specific area to meet irrigation and domestic water needs of the cities of Fujairah and Khor Fakkan. The decline of the groundwater levels may have caused upconing of the saline water as well.

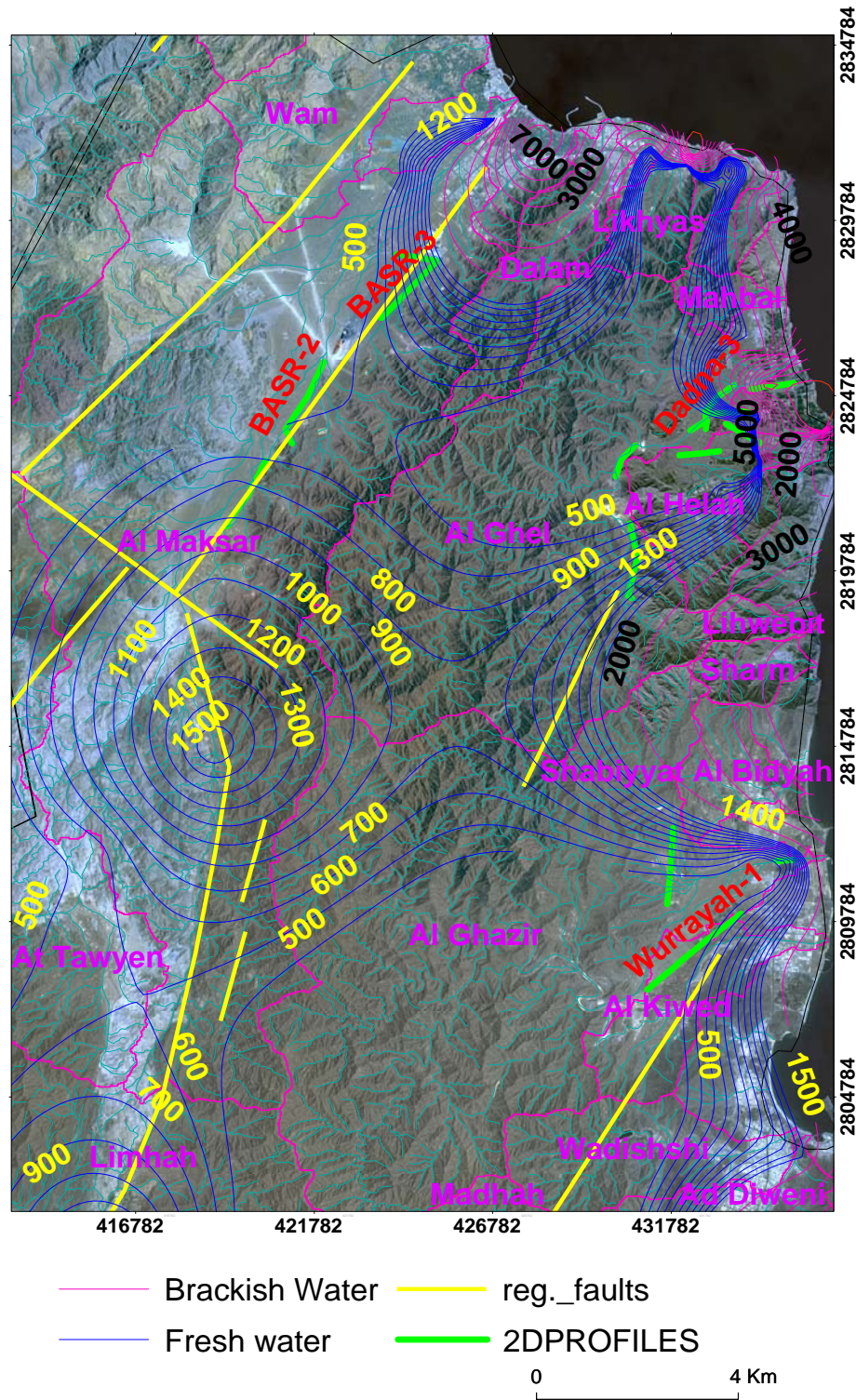


Figure 9.6 Contour map of groundwater salinity in the northern part of the Eastern Coast Region in the UAE. Regional faults (yellow lines) and location of the 2D earth resistivity imaging profiles (green lines) are also shown (Almatari, 2010).

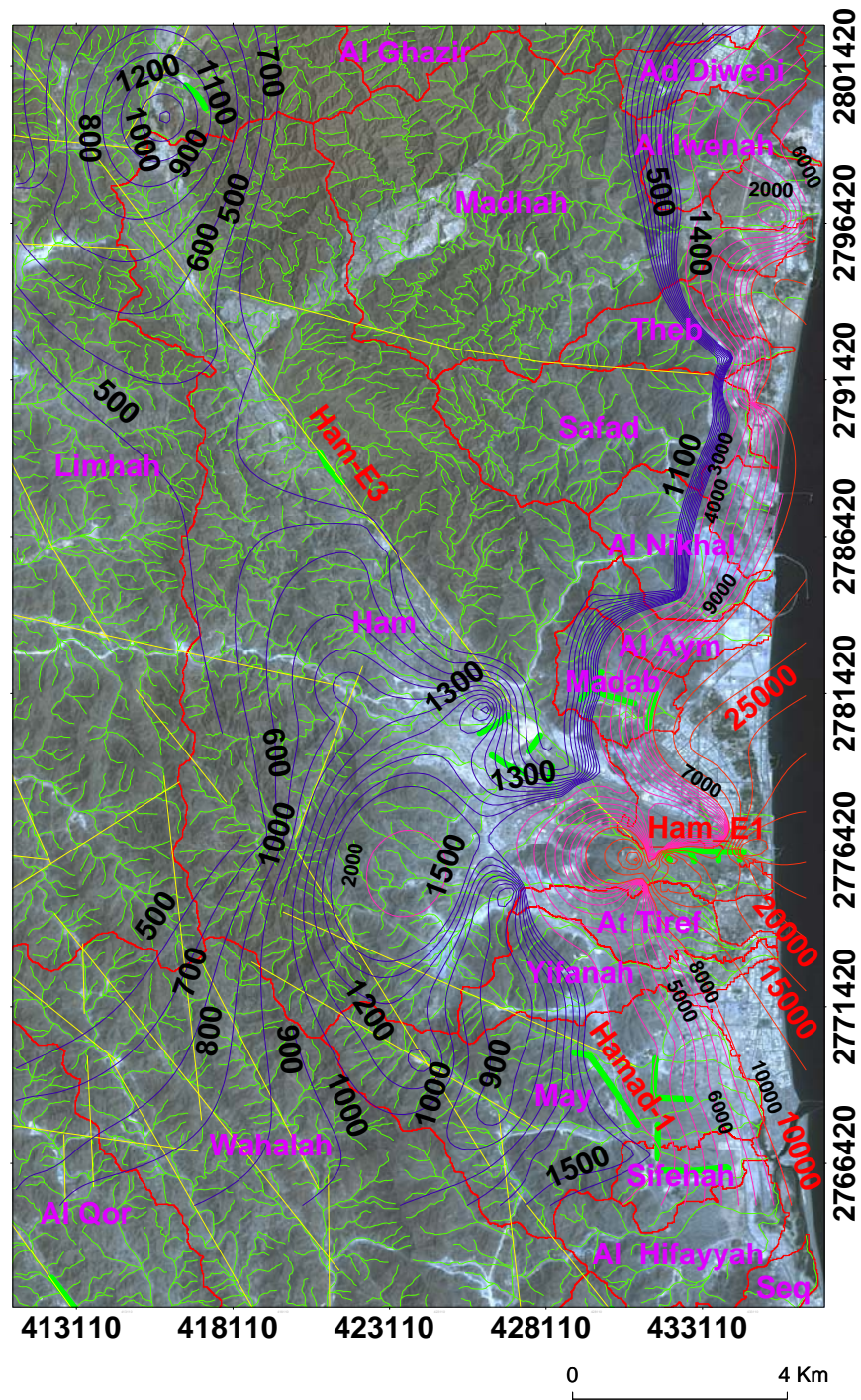


Figure 9.7 Contour map of groundwater salinity in Wadi Ham. Regional faults (yellow lines) and location of the 2D earth resistivity imaging profiles (thick green lines) are also shown (Almatari, 2010).

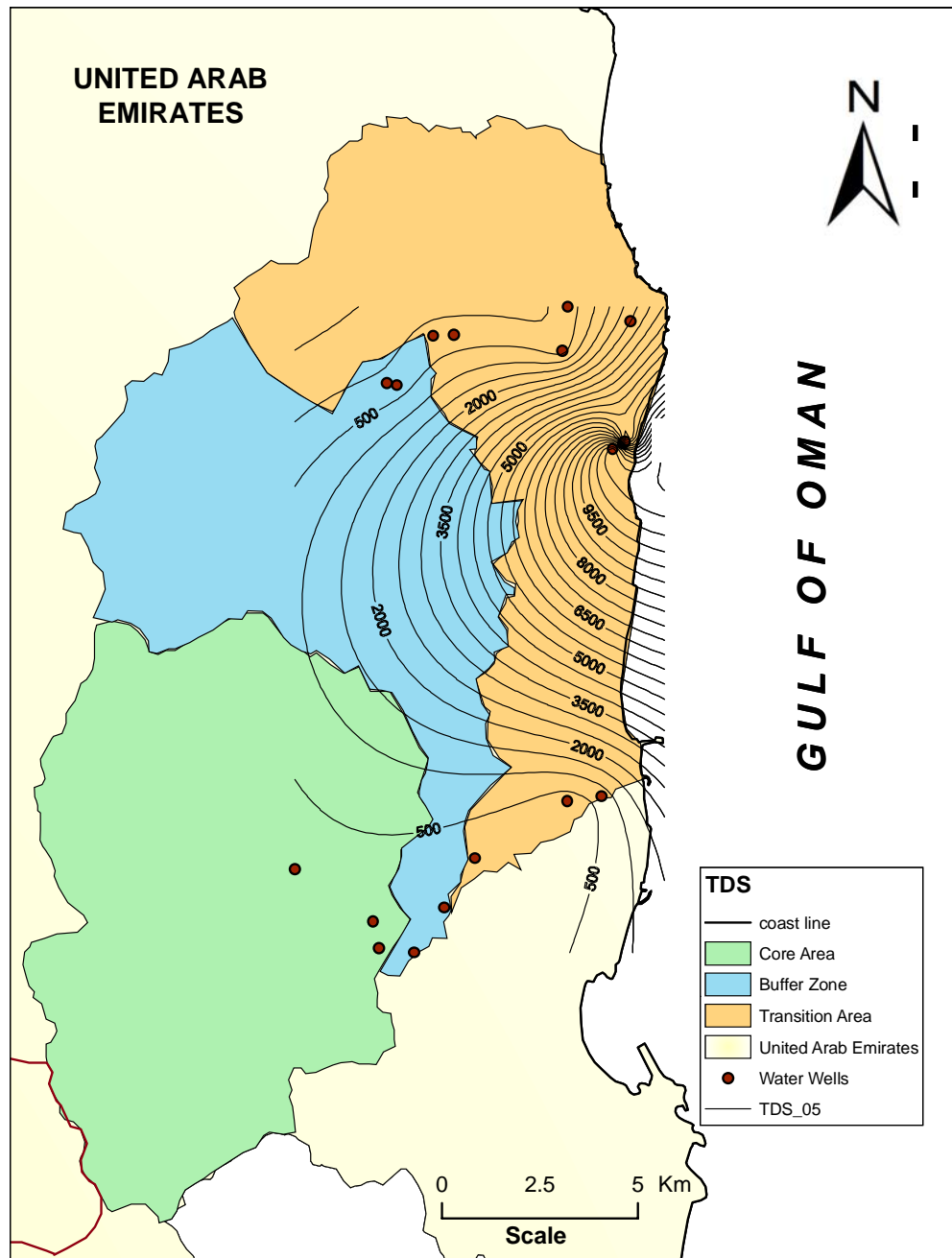


Figure 9.8 Contour map of groundwater salinity in the core area (Wadi Wurayah in Green), buffer zone (Blue) and transition area (Orange), in 2005 (ALHOGARATY).

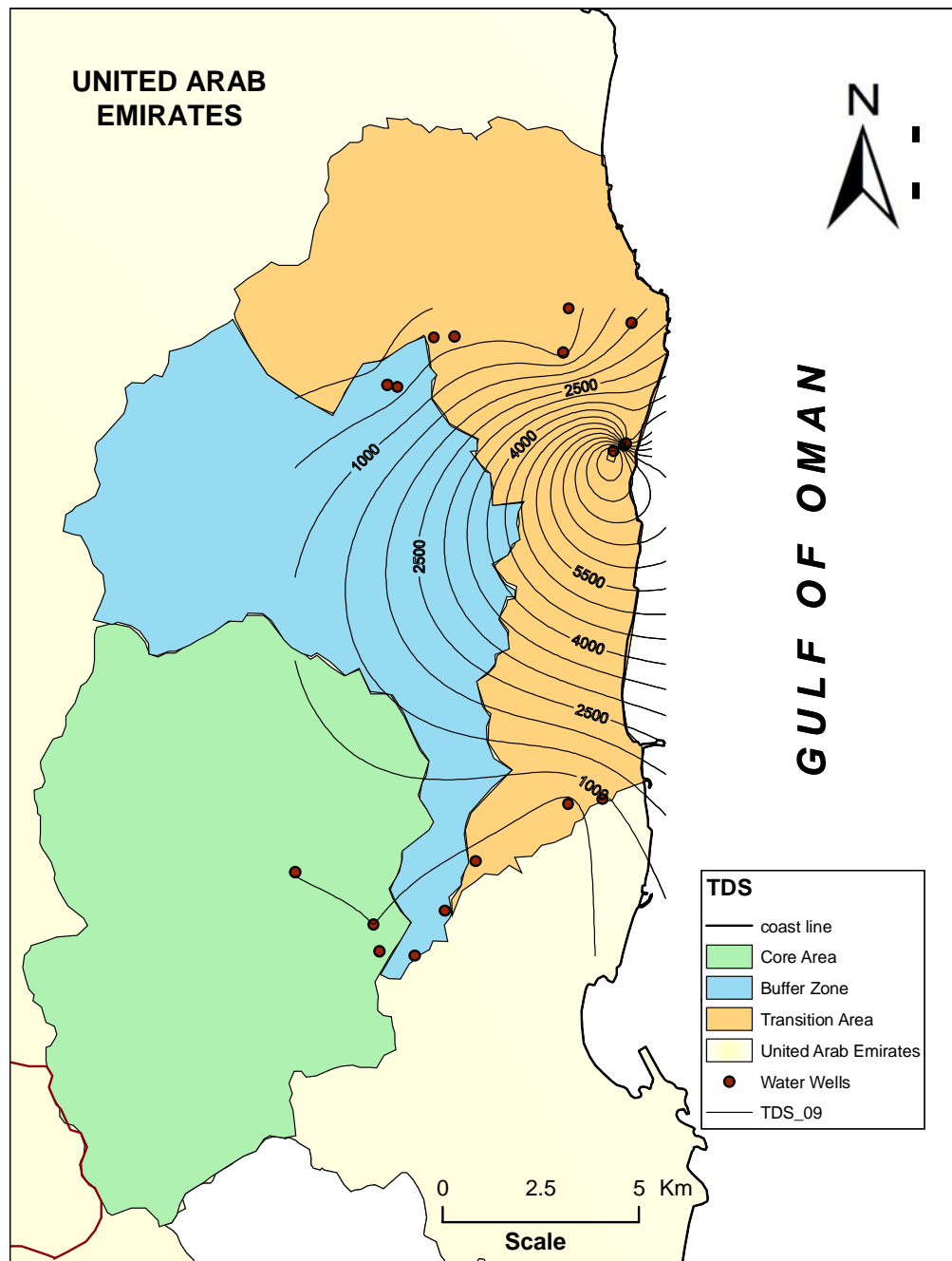


Figure 9.9 Contour map of groundwater salinity in the core area (Wadi Wurayah in Green), buffer zone (Blue) and transition area (Orange), in 2009 (ALHOGARATY).

9.3.2 Hydrogen Ion Concentration

The hydrogen ion concentration (pH) of groundwater is a measure of its acidity or alkalinity. The pH value of water is related to its quality and affects, to a great extent, its suitability for different uses.

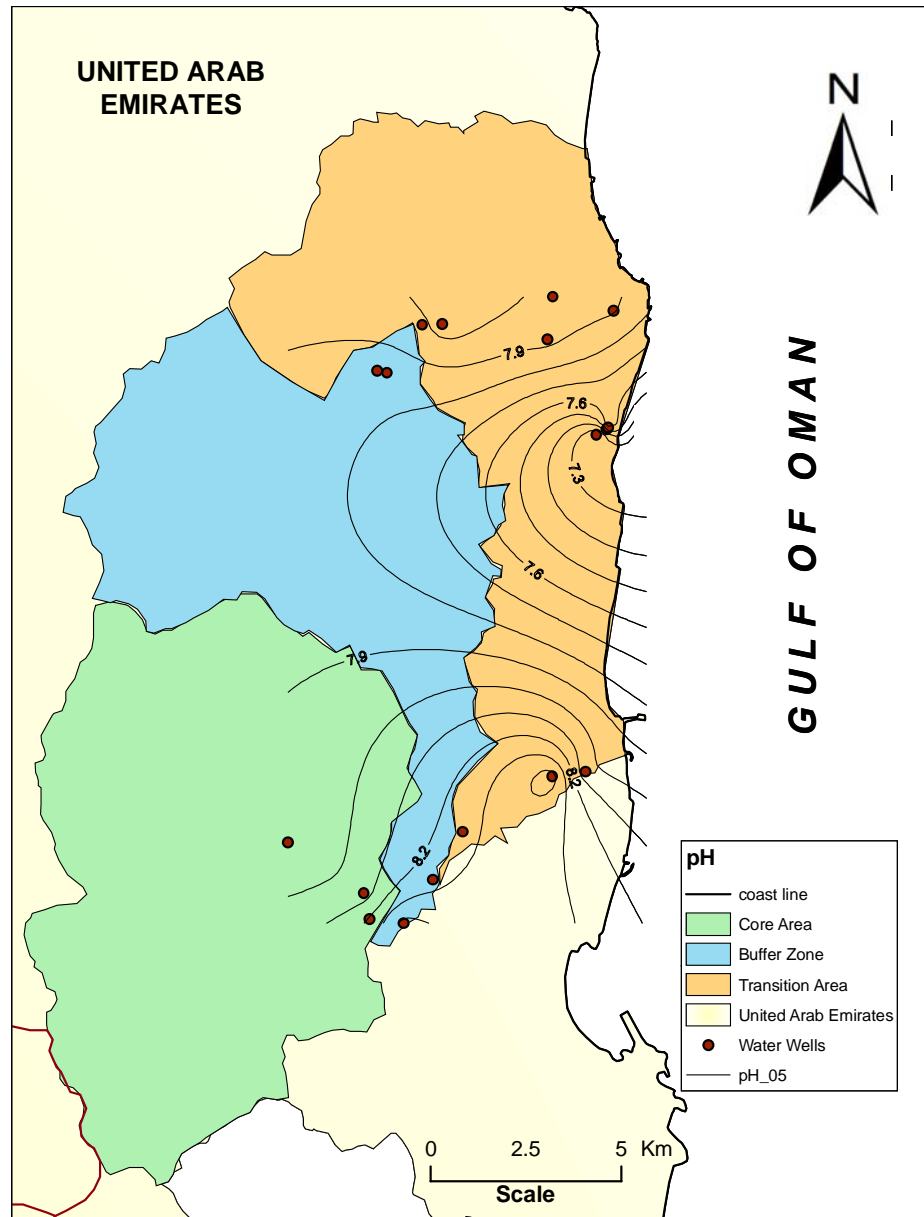


Figure 9.10 Contour map of hydrogen ion concentration for groundwater samples in the core area (Wadi Wurayah in Green), buffer zone (Blue) and transition area (Orange) in 2005 (ALHOGARATY).

The pH is controlled by the amount of dissolved carbon dioxide (CO_2), carbonates (CO_3^{2-}) and bicarbonates (HCO_3^-). The hydrogen ion concentrations (pH) of the collected groundwater samples varied between 7.2 and 8.5 in 2005 and 7.0 and 8.0 in 2009 (Figures 9.10 and 9.11; Table 9.5 and 9.6).

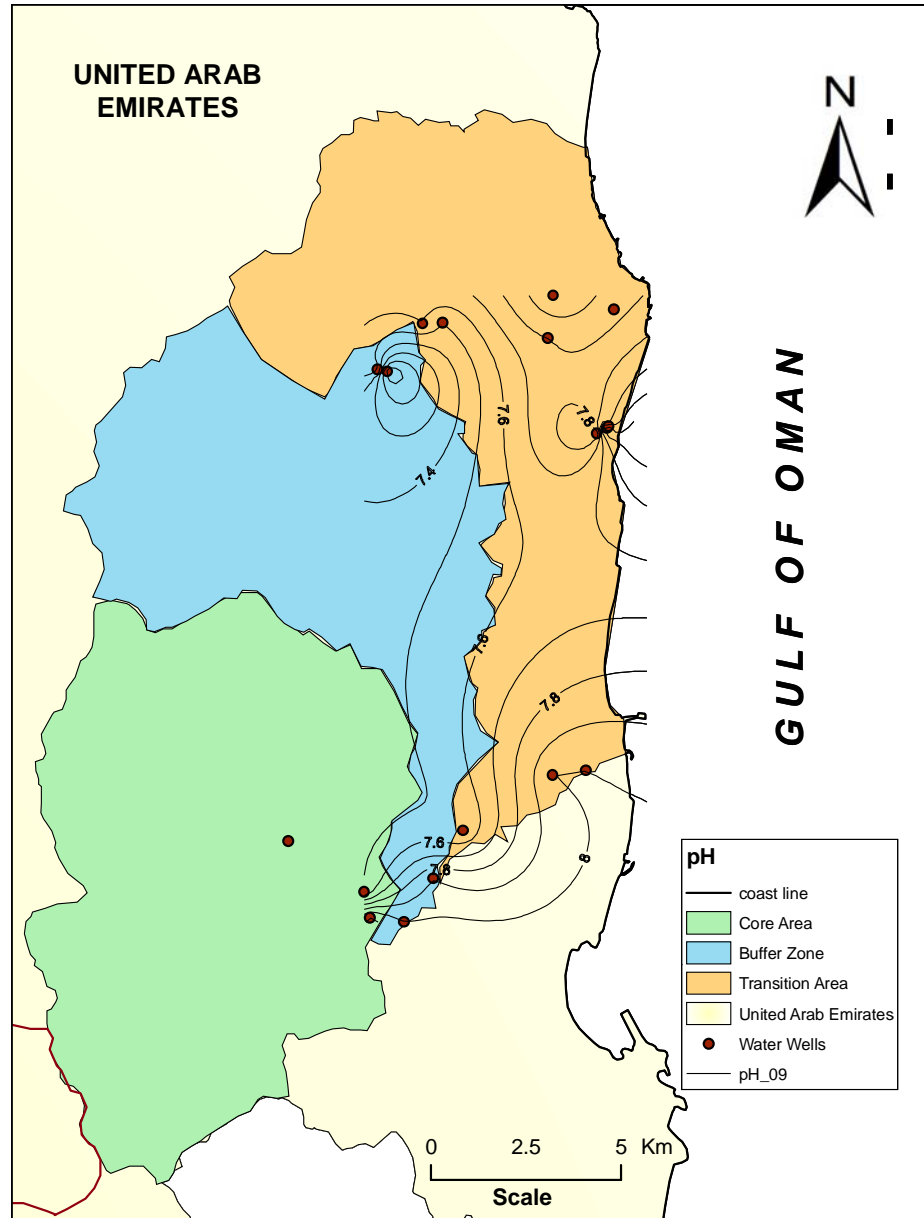


Figure 9.11 Contour map of hydrogen ion concentration for groundwater samples in the core area (Wadi Wurayah in Green), buffer zone (Blue) and transition area (Orange) in 2009 (ALHOGARATY).

This means that the groundwater in the study area varies from slightly acidic, due to dissolution of the various gases in the atmosphere by rainwater and the decay of natural vegetation, to slightly alkaline caused mainly by water enrichment in carbonates (CO_3^{2-}) and bicarbonates (HCO_3^-) ions.

9.3.3 Major Cations

The sequence of cations dominance in groundwater of the Quaternary alluvial aquifer in the Eastern Coast Region of the UAE has the order: $\text{Na}^+ > \text{Mg}^{2+} > \text{Ca}^{2+} > \text{K}^+$ in the Fujairah area, and $\text{Mg}^{2+} > \text{Na}^+ > \text{Ca}^{2+} > \text{K}^+$ in the Wurayah and Zikt areas (Tables 9.5 and 9.6).

9.3.3.1 Calcium

The most common form of calcium in sedimentary rocks is carbonate, particularly as limestone or dolomite, which are absent in the study area (Figure 4.5). However, the Ru'us Al Jibal carbonate sequence overlooks the study area from the northwest. The dissolution of carbonate minerals and carbonate cement yields calcium to groundwater. Calcium is also a major element in ultramafic minerals of the Ophiolite sequence dominating the study area (Figure 4.5).

The calcium ion concentrations in groundwater in the study area in 2005 ranged from 2 mg/l in Zikt (Wells ZKT-3 and ZKT-5; Figure 9.12) to 275 mg/l in Dadinah area (Figure 9.11), Rul Dibba (Well PNT-4). In 2009, calcium ion concentrations ranged from 3 mg/l in the north (Well ZKT-5) to 278 mg/l (Well PNT-4) near the Rul Dibba City (Figure 9.13). The 2005 and 2009 iso-concentration contour maps show a gradual increase in calcium ion from the west to east (Figures 9.12 and 9.13). High calcium ion concentrations are limited to the Rul Dibba area, where excessive groundwater exploitation is taking place and possible salt-water intrusion is affecting groundwater quality.

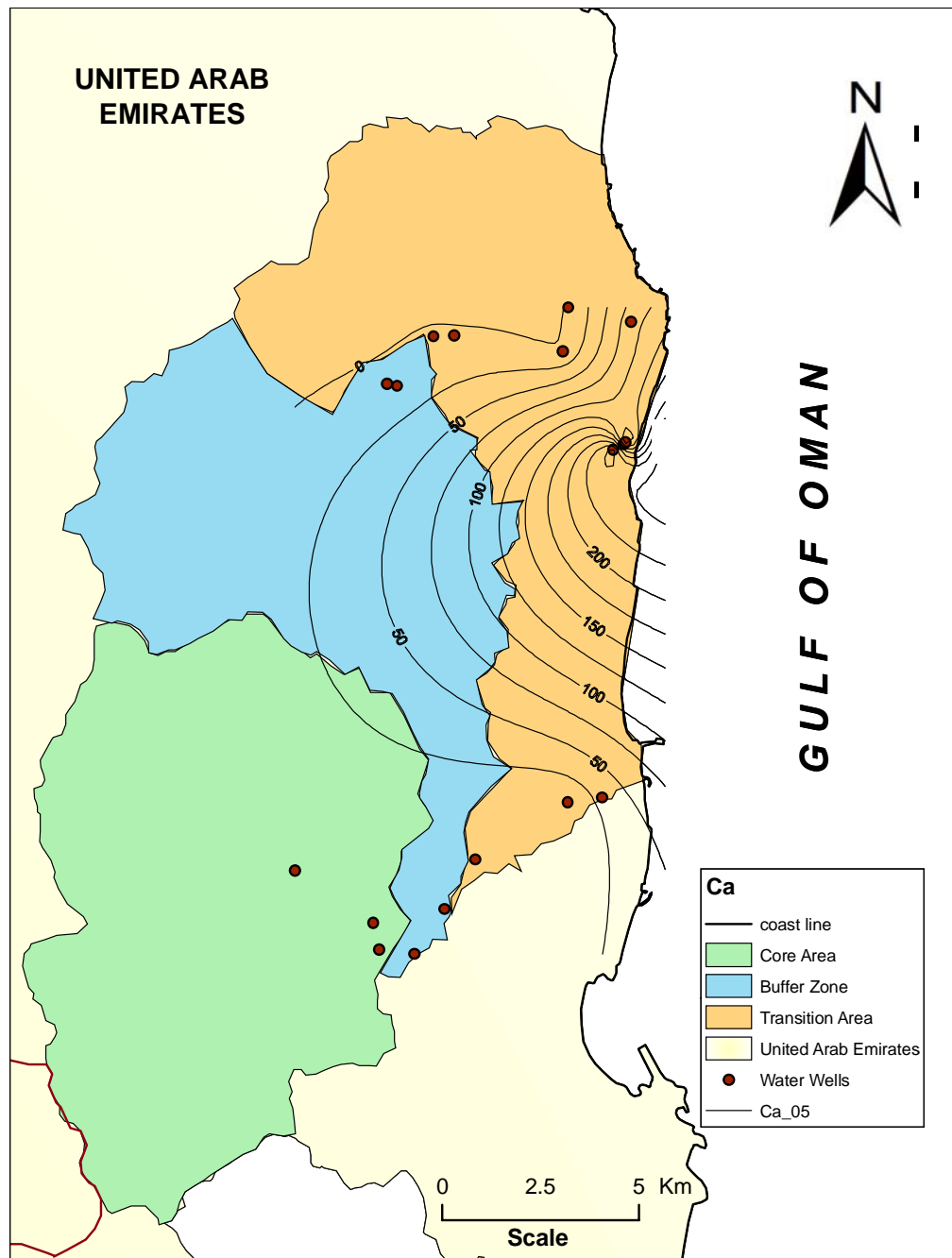


Figure 9.12 Isoconcentration contour map of calcium ion (Ca^{2+}), in mg/l, in groundwater samples collected from the study area in 2005 (ALHOGARATY).

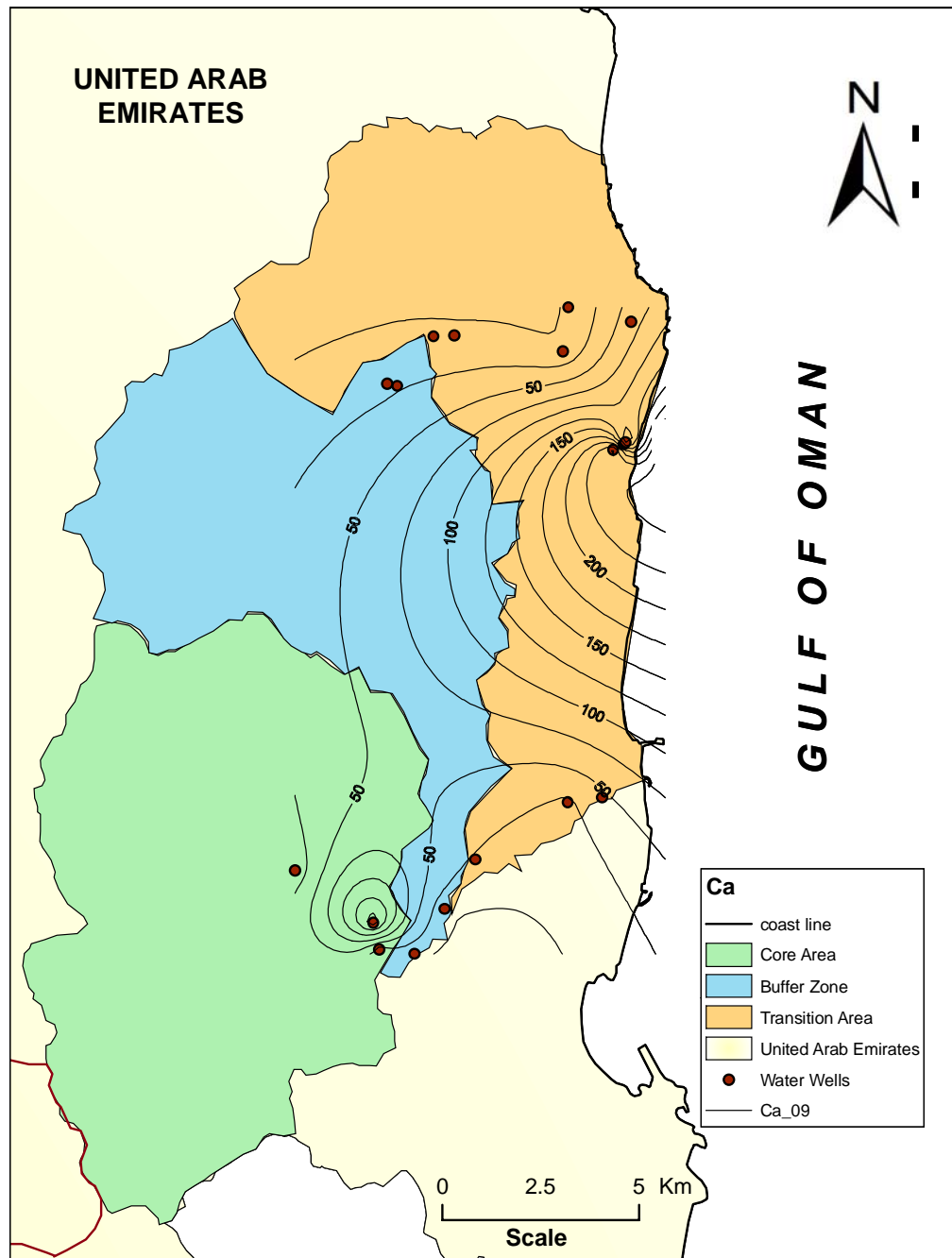


Figure 9.13 Isoconcentration contour map of calcium ion (Ca^{2+}), in mg/l, in groundwater samples collected from the study area in 2009 (ALHOGARATY).

9.3.3.2 Magnesium

The common sources of magnesium in groundwater are dolomite in sedimentary rocks; olivine, biotite, hornblende and augite in igneous rocks; and serpentine, talc and tremolite in metamorphic rocks (Davis and DeWeist, 1966). Both igneous and metamorphic minerals are common in the study area which is dominated by ultramafic Ophiolite (Figure 4.5). The magnesium ion (Mg^{2+}) concentrations in fresh water are generally less than that of calcium because of low geochemical abundance of magnesium (Mathess, 1982). Common concentrations of magnesium range from 1 to 40 mg/l and reach 100 mg/l in water circulating through magnesium-rich rocks. Concentrations of more than 100 mg/l are rarely encountered except in sea water and brines. Because the study area is dominated by ultramafic rocks, Mg^{2+} concentrations >100 mg/l were measured in water samples collected from 4 out of 16 wells in 2005 and 2009 (Tables 9.4 and 9.5). In 2005, magnesium ion (Mg^{2+}) concentration in groundwater within the Eastern Coast Region of the UAE ranged from 17 mg/l in Wadi Wurayah (Well WUR-6) and 652 mg/l in Well (PNT-4) near Rul Dibba. In 2009, Mg^{2+} content ranged from 23 mg/l (Well ZKT-1) in the north to 655 (Well PNT-4) near Rul Dibba. The 2005 and 2009 iso-concentration contour maps show a general increase in Mg^{2+} concentrations from the west to east, in the direction of groundwater flow (Figures 9.14 and 9.15). The high Mg^{2+} concentration in Dadinah area near Rul Dibba attributed to salt water intrusion rather than to dissolution of Mg-rich ophiolitic rocks in Northern Oman Mountains, which represent the main outcrops within the study area.

9.3.3.3 Sodium

The primary source of most sodium ions (Na^+) in natural water is the release of soluble products during the weathering of sodium-bearing minerals particularly plagioclase feldspars which are typical constituents of many igneous rocks. Sodium is also common in evaporites and argillaceous sediments. Sodium ion concentrations in the groundwater within the study area in 2005 ranged from 16 mg/l in the north (Well ZKT-1) and 2,100 mg/l in Dadinah near Rul Dibba (Well PNT-4). In 2009, sodium

ion concentrations ranged from 20 mg/l in Wadi Wurayah west Khor Fakkan (Well WUR-4) to 2,200 mg/l at Dadinah near Rul Dibba (Well PNT-4). The 2005 and 2009 iso-concentration contour maps show a steady increase in Na^+ concentrations from west and southwest to east and northeast (Figures 9.16 and 9.17).

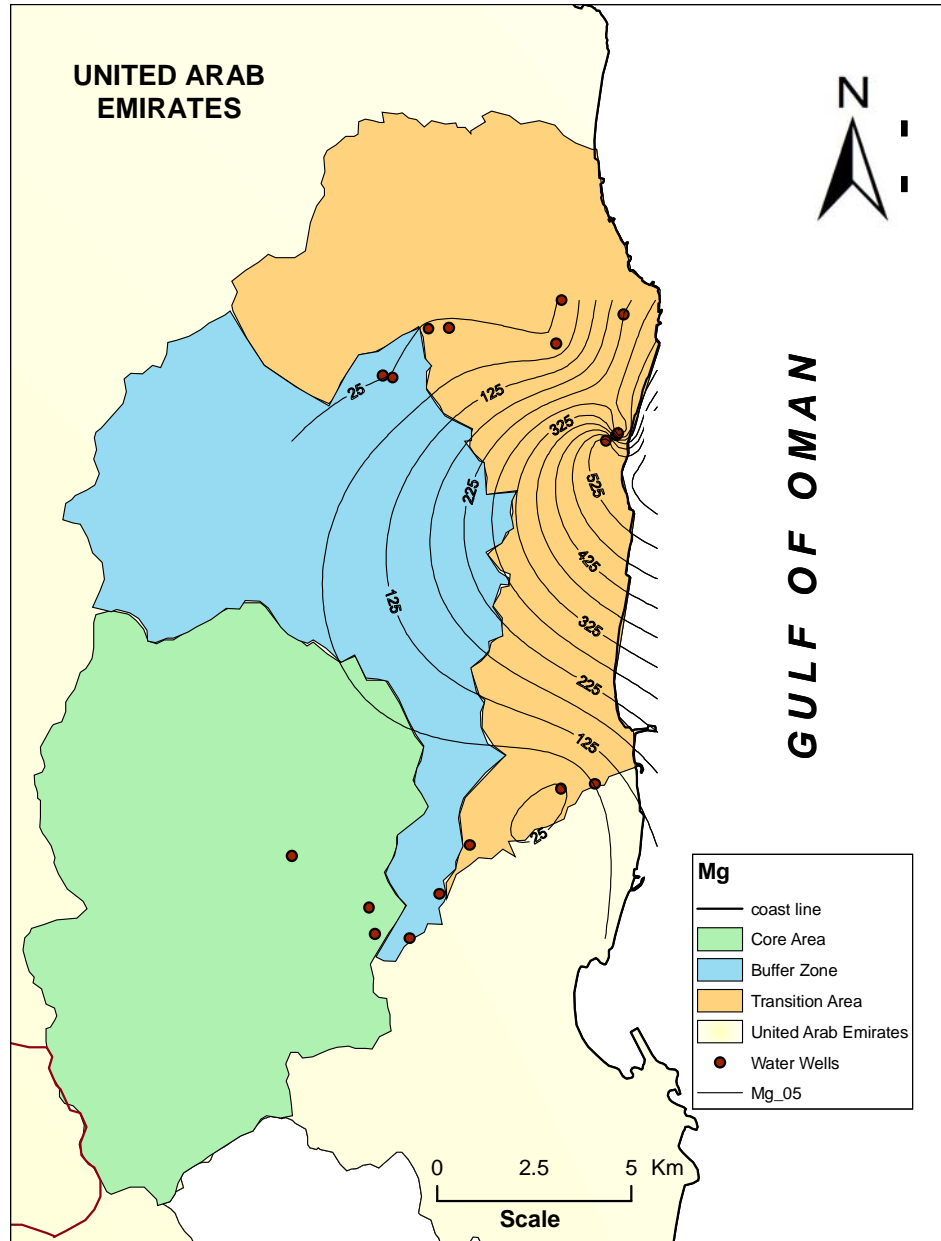


Figure 9.14 Isoconcentration contour map of magnesium ion (Mg^{2+}), in mg/l, in groundwater samples collected from the study area in 2005 (ALHOGARATY).

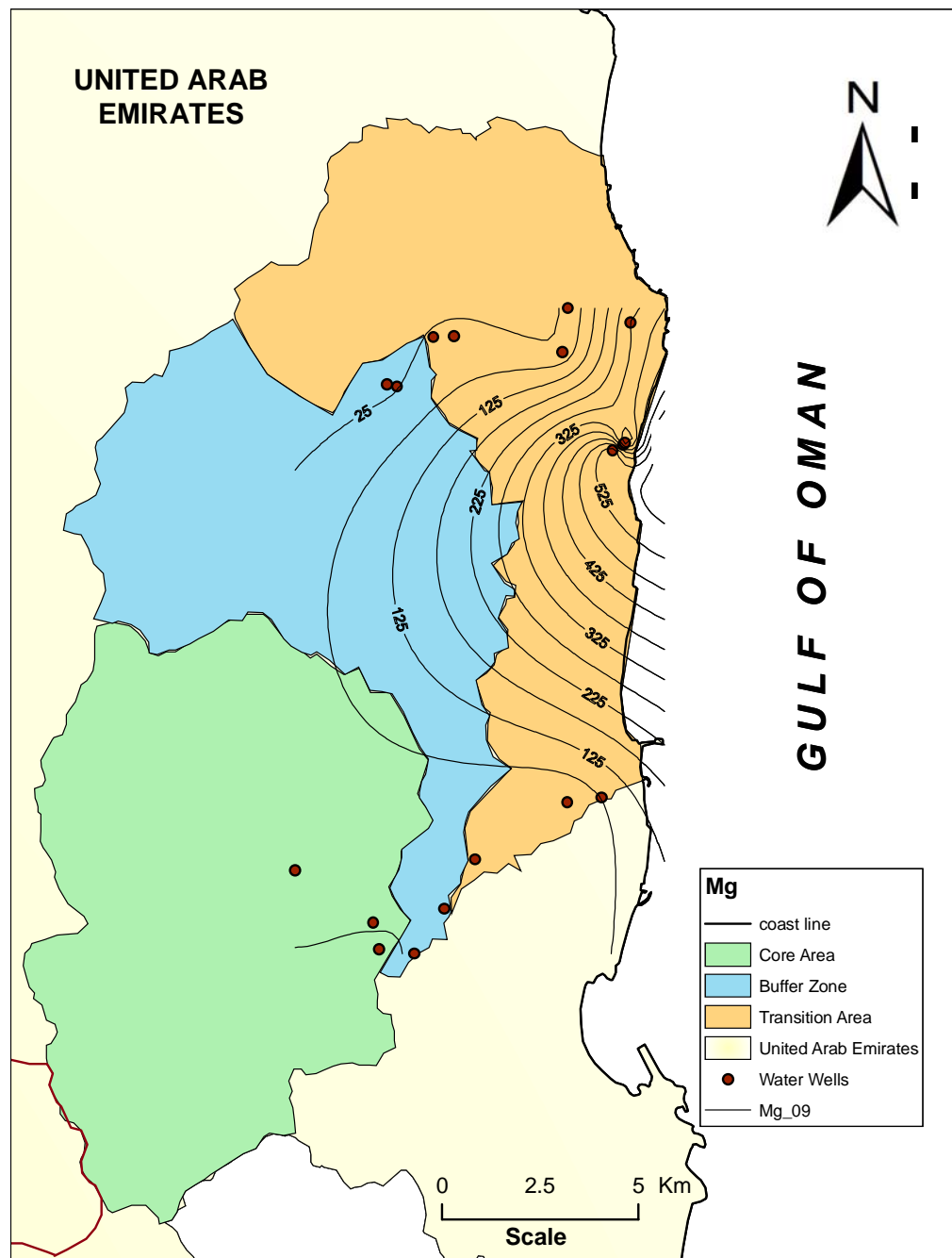


Figure 9.15 Isoconcentration contour map of magnesium ion (Mg^{2+}), in mg/l, in groundwater samples collected from the study area in 2009 (ALHOGARATY).

The Na^+ concentrations are low near the water divide line and increase to the east and west in the direction of groundwater flow. The high levels of Na^+ in Rul Dibba and Khor Fakkan are due to heavy pumping of groundwater for all purposes.

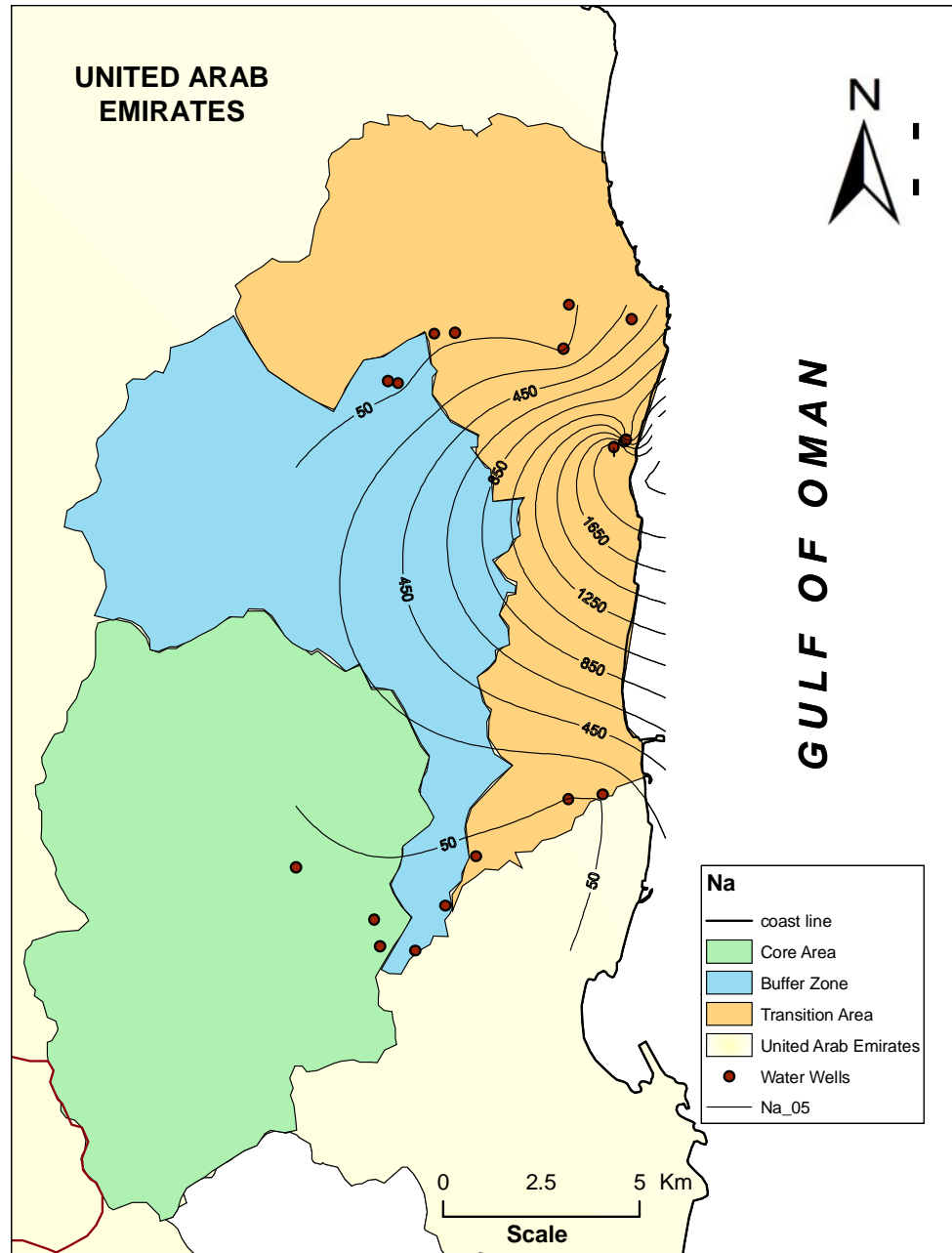


Figure 9.16 Isoconcentration contour map of sodium ion (Na^+), in mg/l, in groundwater samples collected from the study area in 2005 (ALHOGARATY).

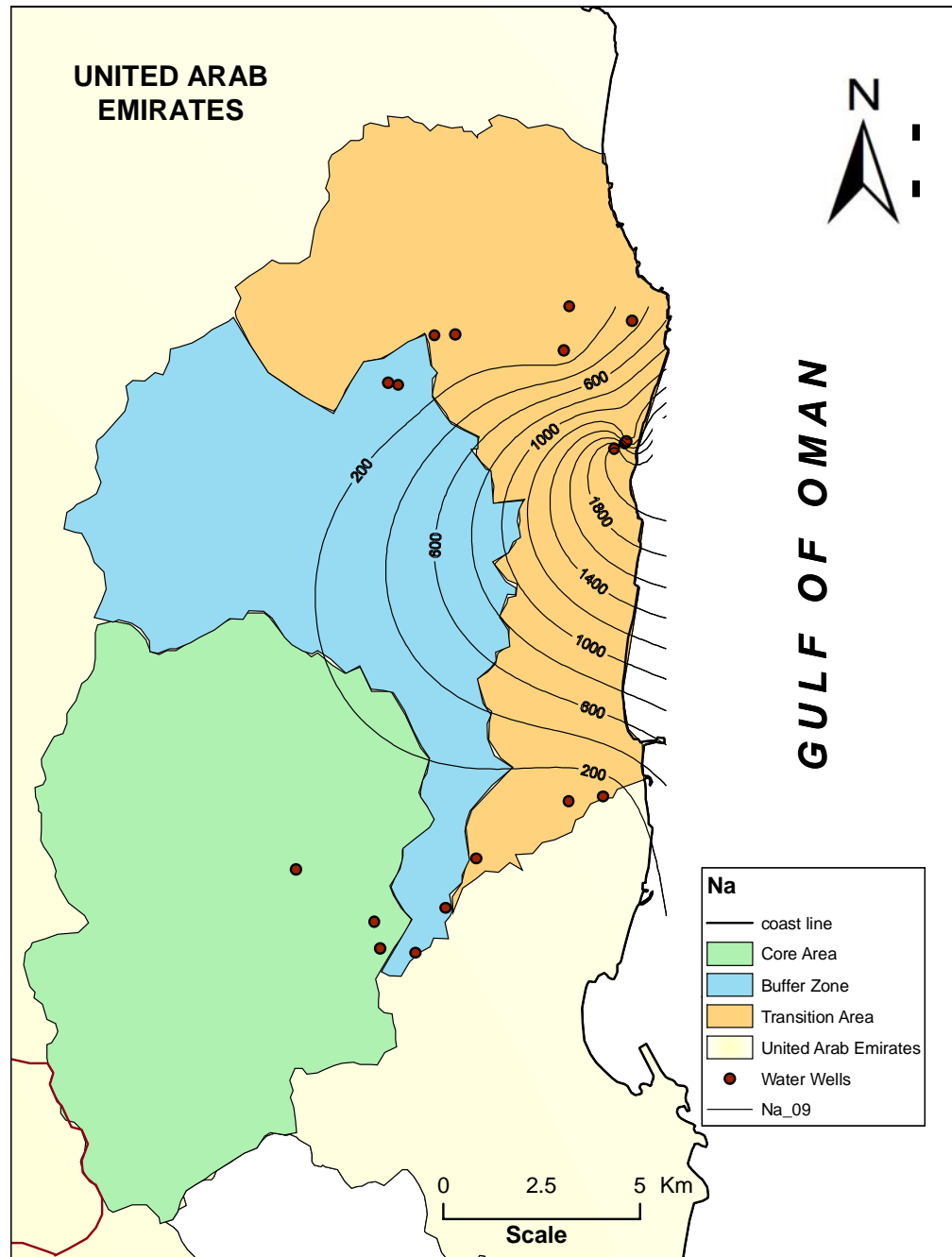


Figure 9.17 Isoconcentration contour map of sodium ion (Na⁺), in mg/l, in groundwater samples collected from the study area in 2009 (ALHOGARATY).

9.3.3.4 Potassium

The most common source of potassium ions (K^+) in groundwater is the weathering of orthoclase, microcline, biotite, leucite and nepheline minerals. Water percolating through evaporite deposits may contain high concentrations of potassium ions (Hem, 1970).

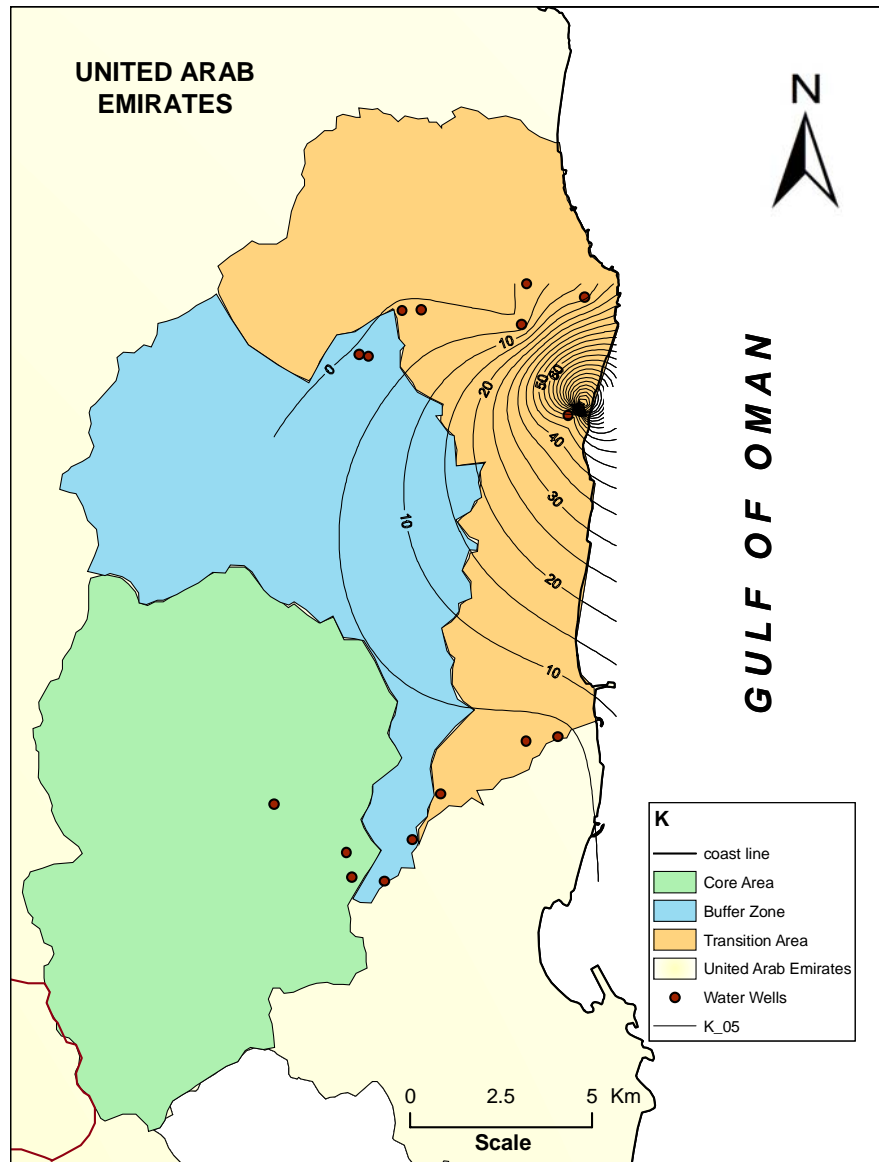


Figure 9.18 Isoconcentration contour map of potassium ion (K^+), in mg/l, in groundwater samples collected from the study area in 2005 (ALHOGARATY).

The K^+ concentration is commonly less than one-tenth the concentration of sodium in natural water because potassium is hardly taken into solution.

The K^+ level in the groundwater within the study area in 2005 ranged from 1 mg/l in several wells in Wurayah and Zikt areas (Wells WUR-3 and WUR-4, and ZKT-1, ZKT-2, ZKT-3 and ZKT-4) to 140 mg/l in Rul Dibba (Well PNT-3).

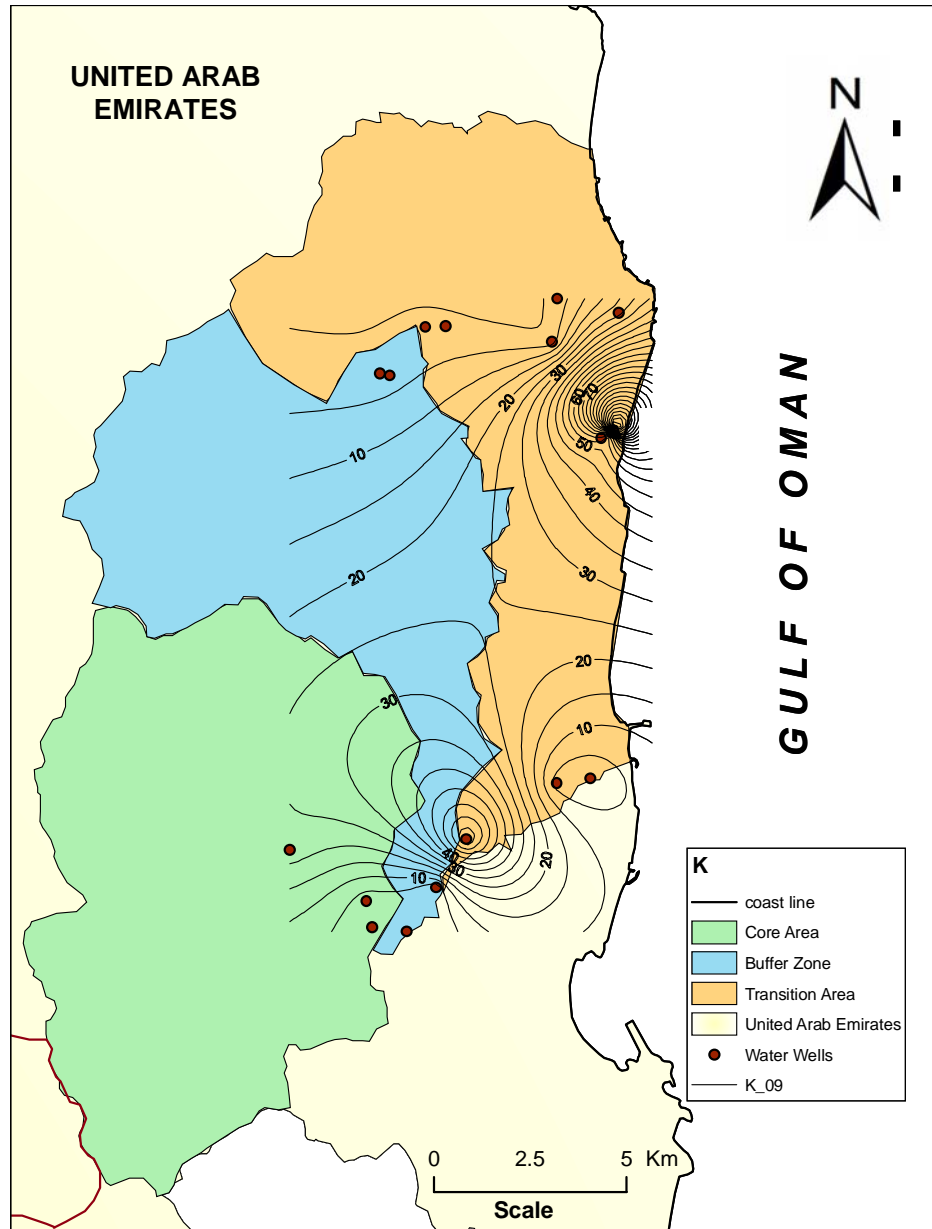


Figure 9.19 Isoconcentration contour map of potassium ion (K^+), in mg/l, in groundwater samples collected from the study area in 2009 (ALHOGARATY).

In 2009, K^+ ranged from 1 mg/l in Wadi Wurayah (Well WUR-4) to 154 mg/l in Rul Dibba (Well PNT-3). The 2005 and 2009 iso-concentration contour maps show a steady increase in K^+ concentration from the west and southwest towards east and northeast (Figures 9.18 and 9.19). The remarkable rise in K^+ level in Well WUR-5 from 3 mg/l in 2005 to 66 mg/l in 2009 can be an analytical error. The K^+ distribution within the study area matches the distribution of other cations.

9.3.4 Major Anions

The sequence of anions dominance in groundwater in the Eastern Coast Region of the UAE has the order: $Cl^- > SO_4^{2-} > HCO_3^-$ in the middle and $HCO_3^- > Cl^- > SO_4^{2-}$ in the north and south (Table 9.5 and 9.6).

9.3.4.1 Bicarbonate

Because the dominant carbon form in natural water (pH 6 - 8) is HCO_3^- (Freeze and Cherry, 1979), the CO_3^{2-} concentration in groundwater within the study area is generally low or absent. Carbonate ions (CO_3^{2-}) commonly exist in water with pH values above 8. Most bicarbonate ions (HCO_3^-) in groundwater are derived from carbon dioxide (CO_2) in the atmosphere, CO_2 in soils and by dissolution of carbonate rocks (Davis and DeWeist, 1966). In the absence of calcareous sediments and carbonate rocks, most of bicarbonate ions in groundwater result from the dissolution of CO_2 within the soil zone by organic decay.

In 2009, sulphate ion concentrations ranged from 34 mg/l in Wadi Wurayah (Well WUR-3) to 1,688 mg/l west of the Rul Dibba Well Field (Well PNT-4). The 2005 and 2009 iso-concentration contour maps show a steady increase in SO_4^{2-} concentrations from the southwest to northeast (Figures 9.22 and 9.23). Sulphate ion levels are low in Wadi Wurayah, Wadi Zikt and near water divide line, increasing towards the Gulf of Oman coast in the east.

Bicarbonate ion concentrations in groundwater within the study area in 2005 ranged from 110 mg/l in Wadi Zikt in the north (Well ZKT-3) to 509 mg/l near Rul Dibba (Well PNT-2). In 2009, bicarbonate ion concentrations in the study area ranged from

123 mg/l in Wadi Zikt (Well Zikt-3) to 501 mg/l at Dadinah near Rul Dibba (Well PNT-2).

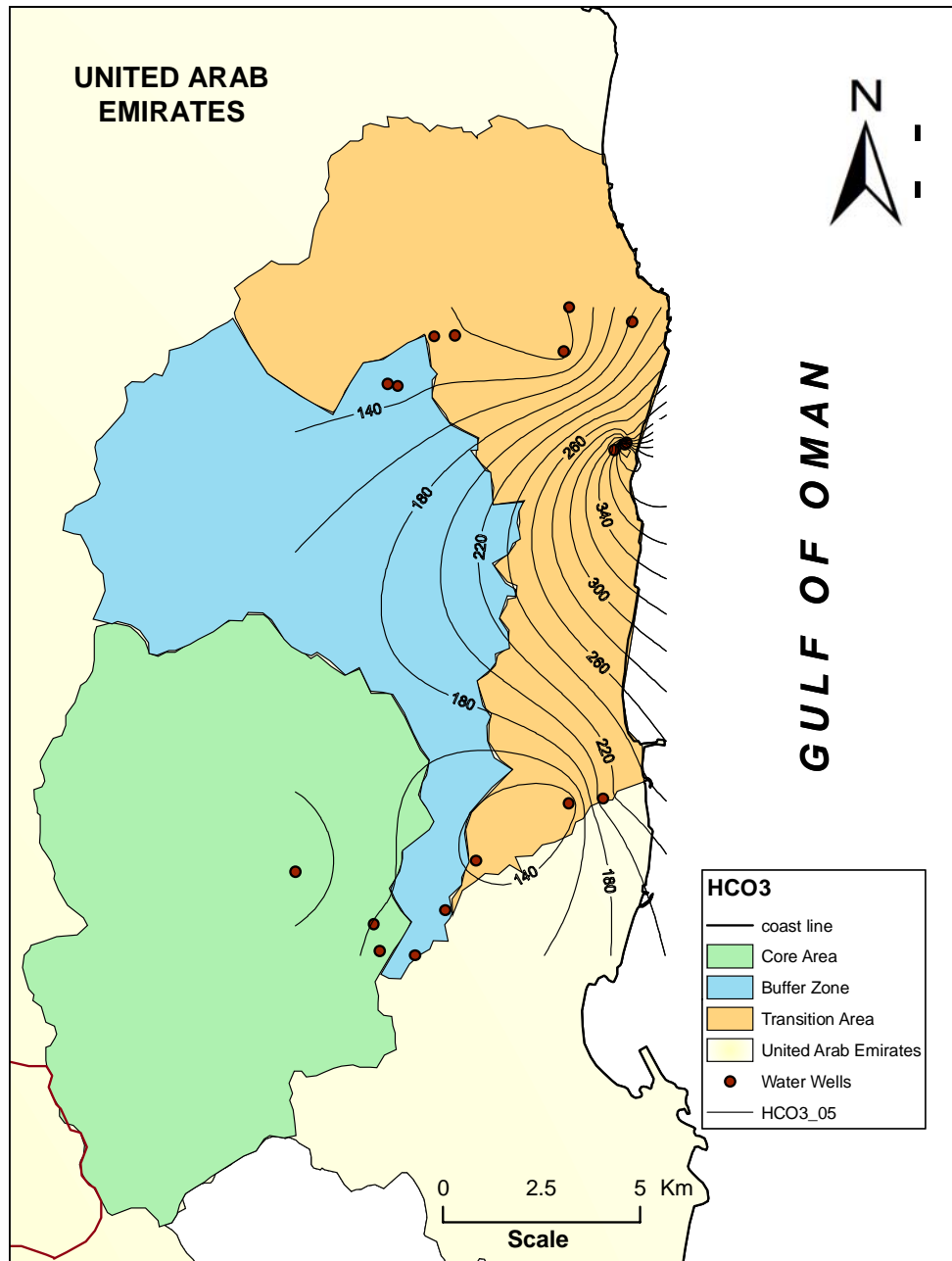


Figure 9.20 Isoconcentration contour map of bicarbonate ion (HCO_3^-), in mg/l, in groundwater samples collected from the study area in 2005 (ALHOGARATY).

The 2005 and 2009 iso-concentration contour maps show a steady decrease in HCO_3^- concentrations from the west to east, in the direction of groundwater flow (Figures 9.20 and 9.21). The HCO_3^- levels are high near the water divide line, decreasing towards the Gulf of Oman coast. Water wells tapping wadi channels or lineament-affected areas can have high HCO_3^- levels.

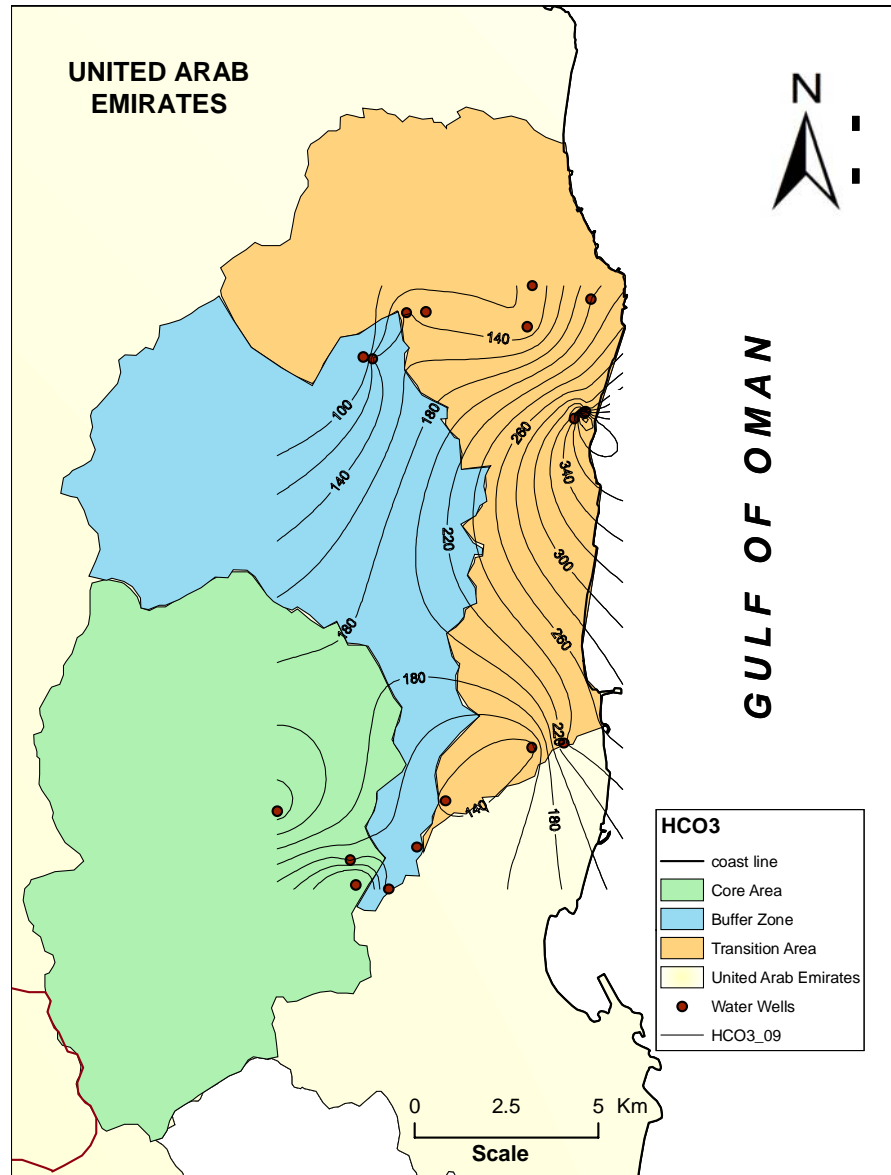


Figure 9.21 Isoconcentration contour map of bicarbonate ion (HCO_3^-), in mg/l, in groundwater samples collected from the study area in 2009 (ALHOGARATY).

9.3.4.2 Sulphate

Sulphate is widely distributed in a reduced form in igneous and sedimentary rocks as metallic sulphides (Hem, 1970). Sulphate ions (SO_4^{2-}) are derived from gypsum ($\text{CaSO}_4 \cdot 2\text{H}_2\text{O}$) or anhydrite (CaSO_4) in sedimentary rocks. Sulphate ion contents in the study area in 2005 ranged from 37 mg/l in Wadi Wurayah and Wadi Zikt (Wells WUR-6 and ZKT-2) to 1708 mg/l near Rul Dibba (Well PNT-4).

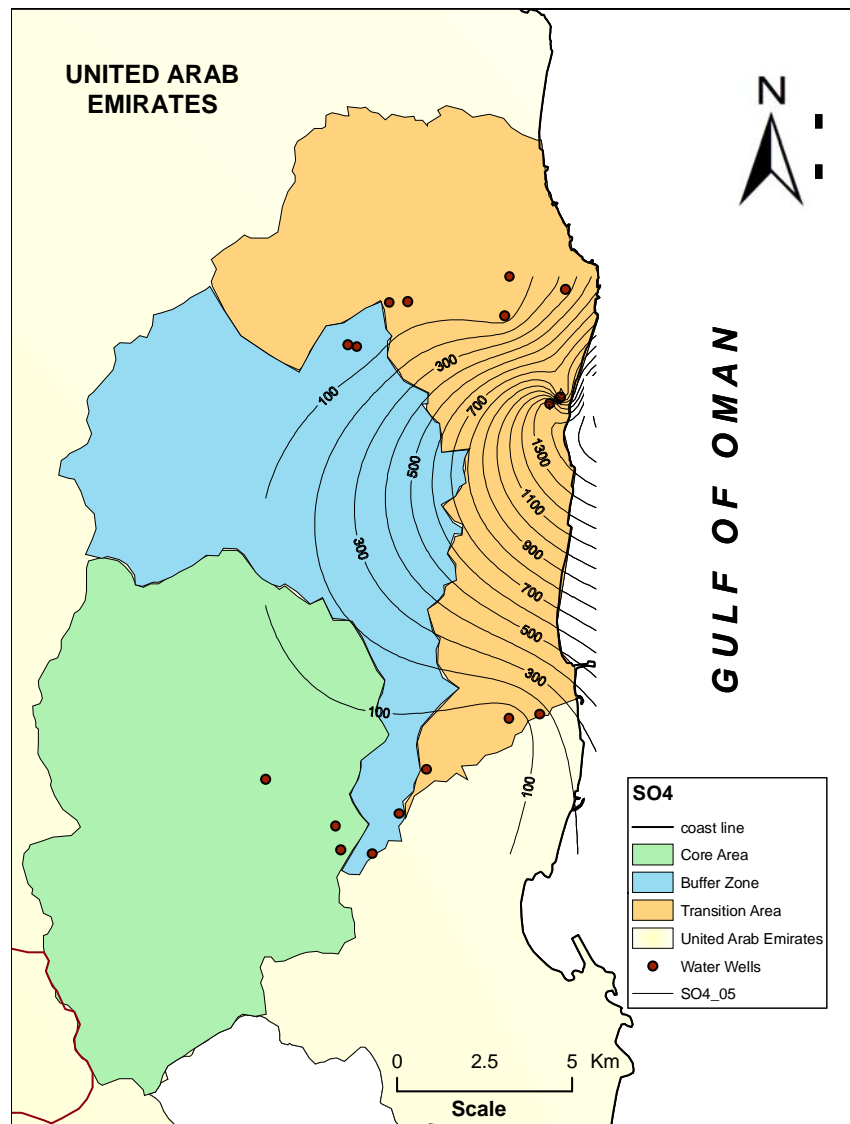


Figure 9.22 Isoconcentration contour map of sulphate ion (SO_4^{2-}), in mg/l, in groundwater samples collected from the study area in 2005 (ALHOGARATY).

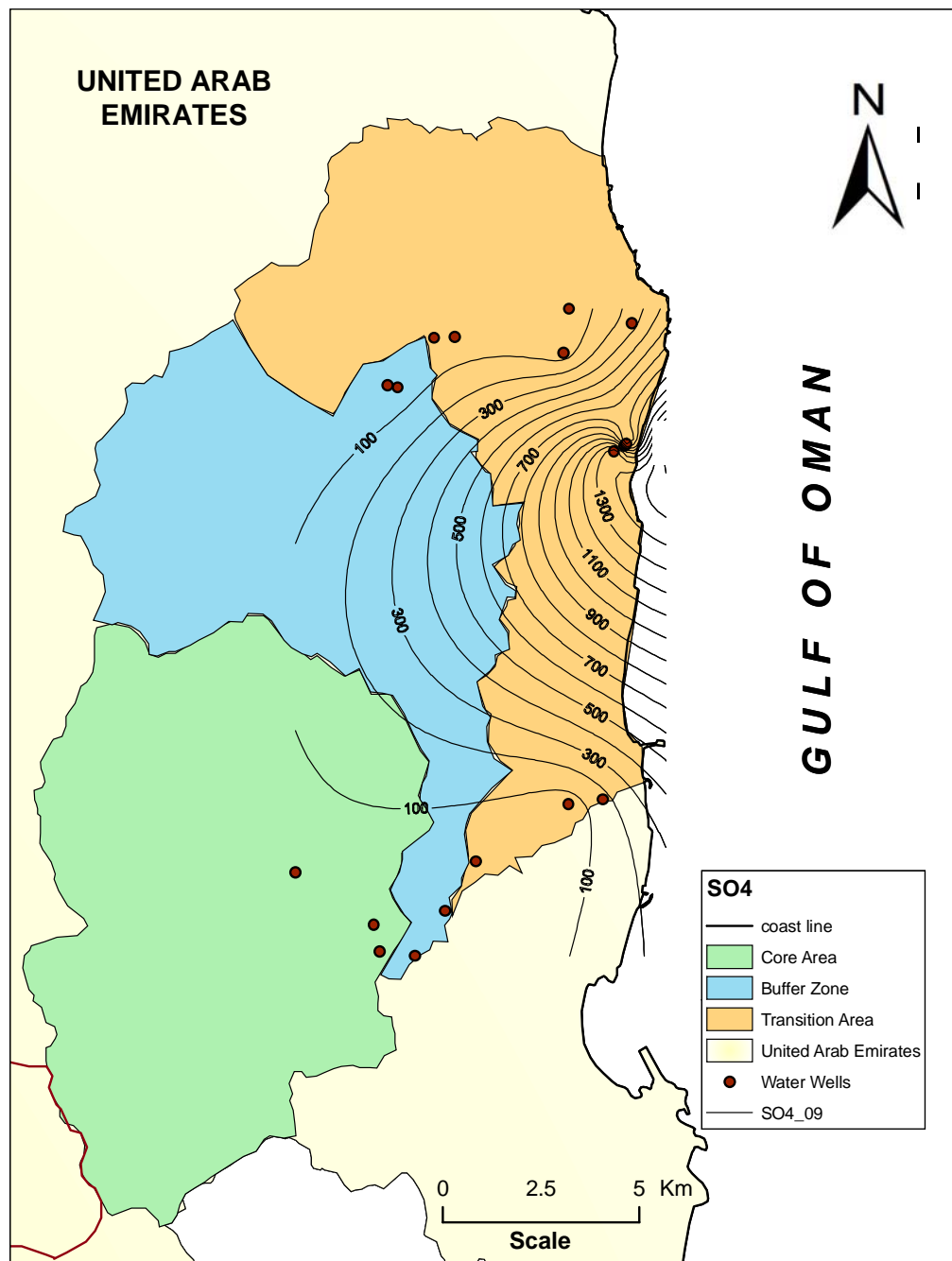


Figure 9.23 Isoconcentration contour map of sulphate ion (SO_4^{2-}), in mg/l, in groundwater samples collected from the study area in 2009 (ALHOGARATY).

9.3.4.3 Chloride

The chloride ion (Cl^-) is the most widely distributed in natural water. Some evaporites provide high concentrations of Cl^- to normal groundwater (El-Shami, 1982).

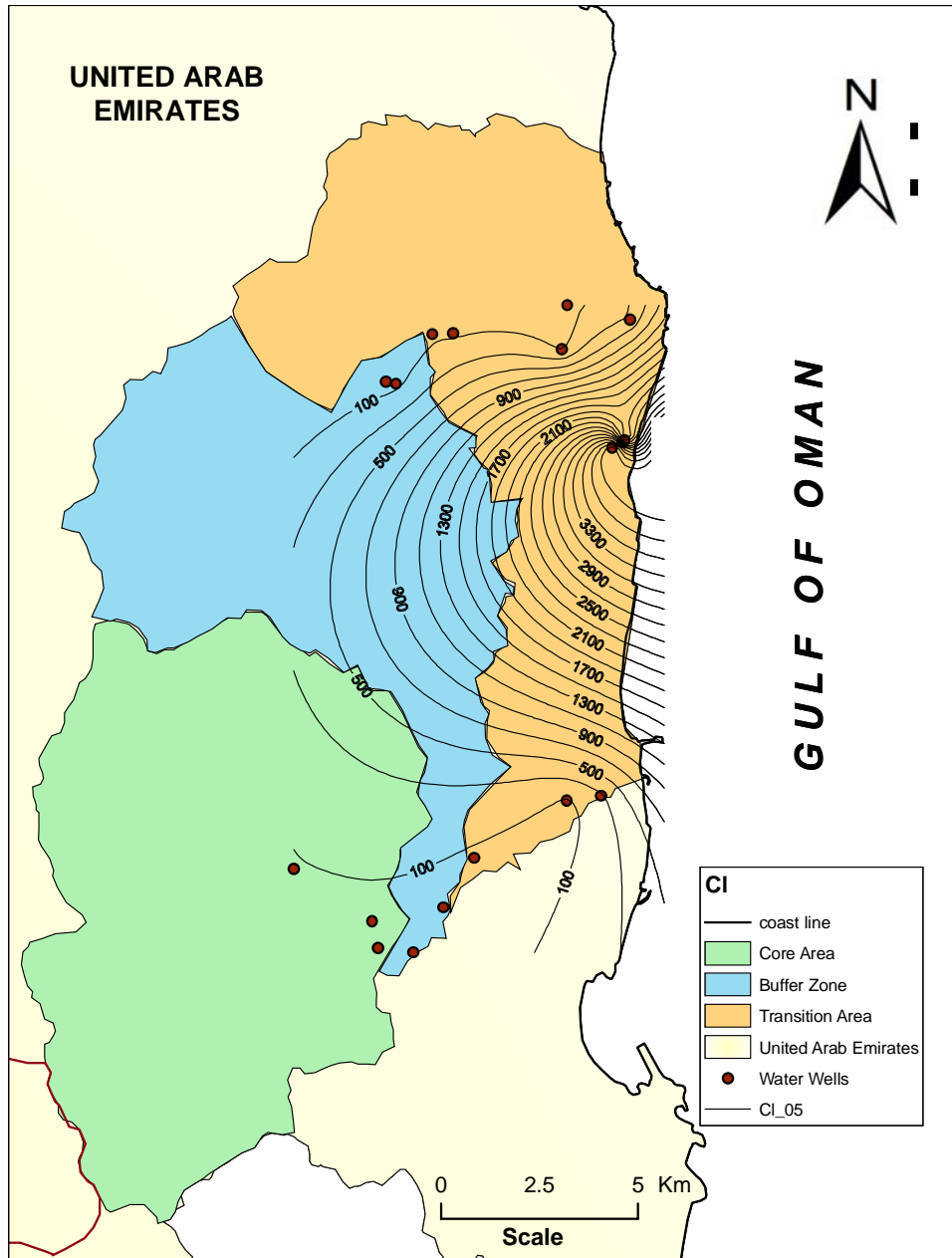


Figure 9.24 Isoconcentration contour map of chloride ion (Cl^-), in mg/l, in groundwater samples collected from the study area in 2005 (ALHOGARATY).

Most Cl^- in groundwater comes from four different sources; ancient sea water entrapped in sediment, solution of halite and related minerals in evaporite deposits and the solution of dry fallout from the atmosphere, particularly in arid regions (Davis and DeWeist, 1966).

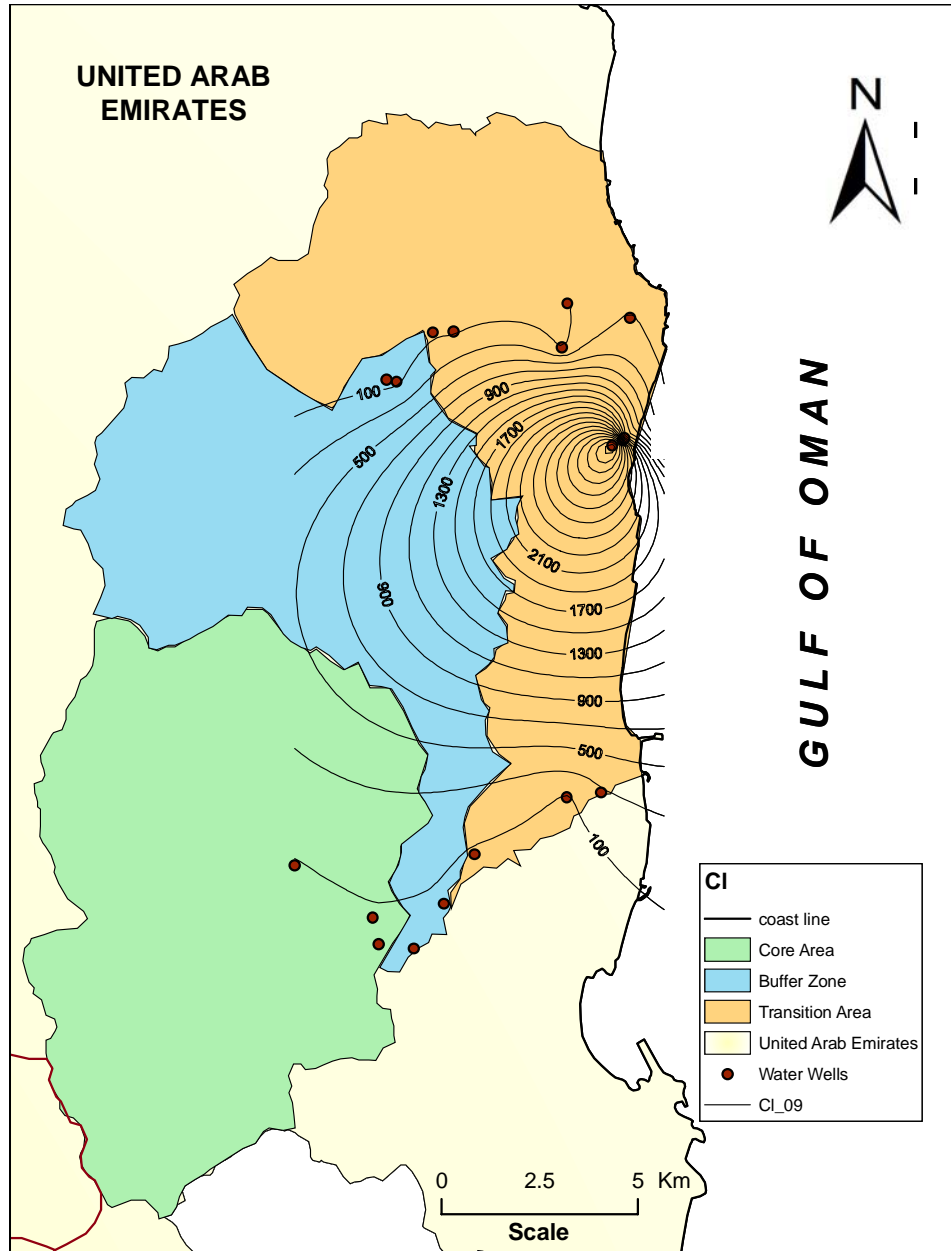


Figure 9.25 Isoconcentration contour map of chloride ion (Cl^-), in mg/l, in groundwater samples collected from the study area in 2009 (ALHOGARATY).

Chloride ion concentrations in groundwater within the study area in 2005 ranged from 53 mg/l in Wadi Zikt and Wadi Wurayah (Wells WUR-3 and ZKT-1) to 4,213 mg/l in Rul Dibba (Well PNT-4). In 2009, the chloride ion ranged from 51 mg/l in Wadi Wurayah (Well WUR-3) to 4,100 mg/l west of Dadinah (Well PNT-5). The 2005 and 2009 iso-concentration contour maps show a steady increase in Cl^- concentrations from the west to east and northeast (Figures 9.24 and 9.25). Chloride-ion contents are low in the west close to the water divide line, increasing towards the Gulf of Oman in the direction of groundwater flow. The high Cl^- at Dadinah area is related to heavy groundwater exploitation for all agricultural purposes.

9.3.5 Dissolved Salts

The calculated groundwater dissolved salts in groundwater of the study area are consistent with the prevailing geological and hydrogeological conditions and evolve in the direction of groundwater flow, according to the Chebotarev series (Freeze and Cherry, 1979).

Table 9.8 Calculated major dissolved salts (%) groundwater in the Eastern Coast Region of the UAE in 2009 (ALHOGARATY).

No.	Easting	Northing	KCl	NaCl	MgCl_2	MgSO_4	$\text{Mg}(\text{HCO}_3)_2$	$\text{Ca}(\text{HCO}_3)_2$
1	435578	2820142	1	67	6	18	2	6
2	435616	2820195	6	64	1	20	3	5
3	436630	2820161	1	57	16	17	0	4
4	435309	2820013	1	59	17	15	0	4
5	427193	2809291	1	22	14	15	39	8
6	429201	2807961	1	27	9	17	38	9
7	430235	2807161	1	23	9	17	41	10
8	431007	2808298	1	24	10	16	42	8
9	431798	2809560	2	29	10	19	37	4
10	434154	2811024	2	42	0	4	35	6
11	435021	2811140	1	23	29	22	9	15
12	429811	2821628	1	21	14	14	38	13
13	430736	2822891	1	23	16	16	39	6
14	434025	2822517	1	24	19	17	37	3
15	431261	2822918	1	24	17	17	38	4
16	434166	2823637	1	32	12	16	37	3

The compositions of the groundwater within the study area vary from north to south. The predominance of groundwater dissolved salts changes from magnesium

bicarbonate in Wadi Zikt in the north to sodium chloride in Dadinah in the middle to magnesium bicarbonate again in Wadi Wurayah in the south. Magnesium chloride water type was dominant in one well at Wadi Wurayah (WUR-7; Table 9.6). The sodium chloride water type dominating groundwater in the Dadinah area can be attributed to salt water intrusion from the Gulf of Oman (Figure 9.30).

The spatial distribution of hypothetical salt combinations reflects the influence of both natural hydrogeologic conditions and human-related activities. The $\text{Ca}(\text{HCO}_3)_2$ salt is dominate in the Wadi Zikt and Wadi Wurayah basins in the northern and southern parts of the study area (Figure 9.26).

The Mg-rich ultramafic rocks are the main rock types within the study area, therefore the $\text{Mg}(\text{HCO}_3)_2$ is the most dominant salt throughout the region. The percentage of $\text{Mg}(\text{HCO}_3)_2$ reaches 42% in Wadi Wurayah (Well WUR-4), decreasing to 2% in Dadinah well field (Figure 9.27).

Two dominance of MgSO_4 salt prevailed all over the study area, except the area around Well WUR-6 (Figure 9.28), which is characterized by NaCl followed by $\text{Mg}(\text{HCO}_3)_2$ water types (Table 9.8). The MgSO_4 iso-percentage contours decrease from 20% in Dadinah to 4% near the outlet of wadi Wurayah (Figure 9.28).

The MgCl_2 salt is the fourth dominant salt within the study area, reaching maximum of 29% in WUR-7 well and minimum of 1% in Dadinah (Well PNT-3). Generally, the dominance of the MgCl_2 salt decreased from the west to east (Figure 9.29).

The NaCl dominate the eastern strip of the study area parallel to the Gulf of Oman coast (Figure 9.30). The dominance of NaCl salt generally increases from the west to east, in the direction of groundwater flow. Local increases in NaCl salt reflect the influence of salt water intrusion from the Gulf of Oman into the eastern gravel aquifer within the study area (Sherif et al., 2005).

The KCl is the least dominant salt within the study area (Figure 9.30), reaching maximum concentration in Dadinah (6% Well PNT-3) and decreases throughout the Wurayah and Zikt drainage basins (between 1 and 2%; Table 9.8).

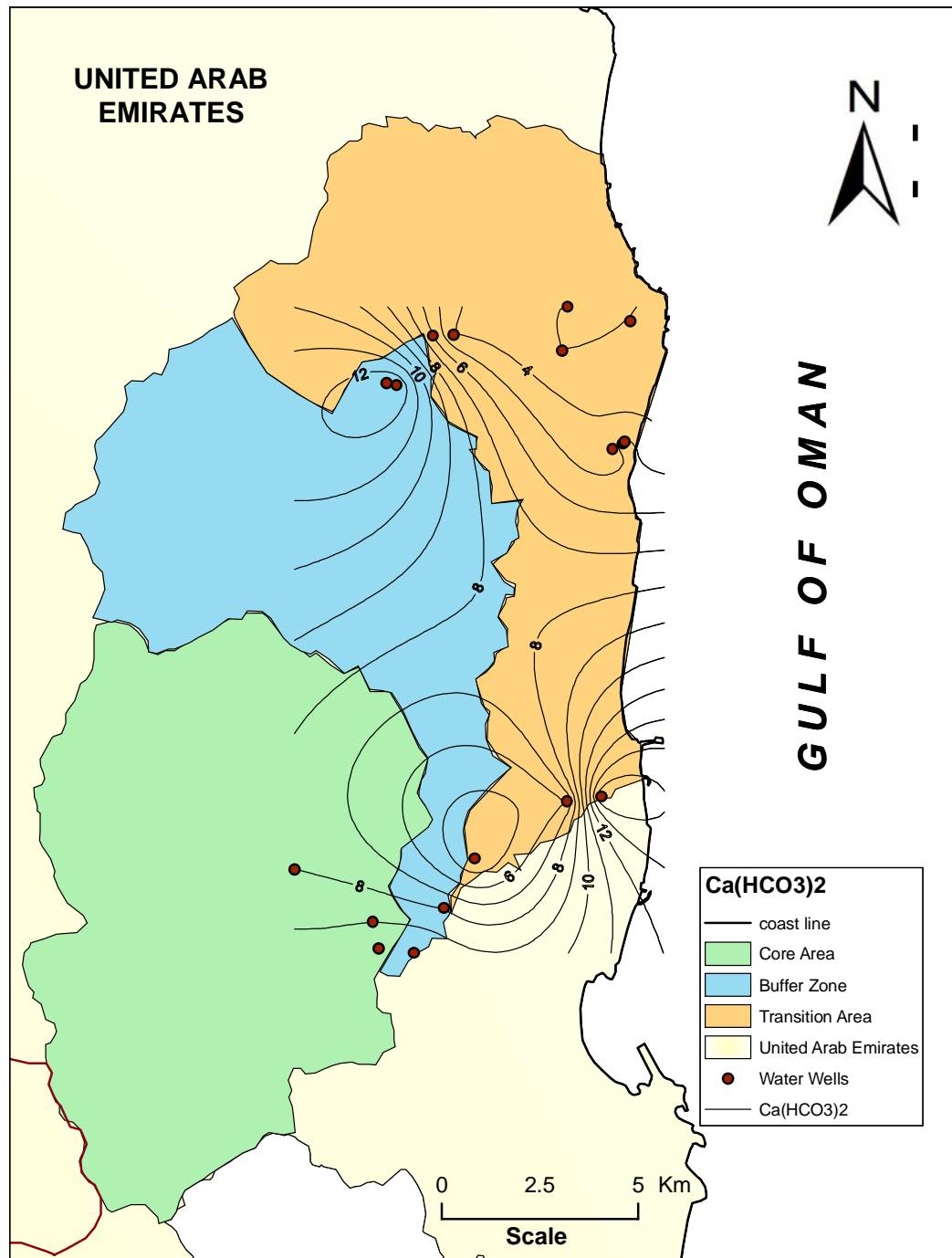


Figure 9.26 Dominance of the $\text{Ca}(\text{HCO}_3)_2$ groundwater dissolved salt (%) in the eastern gravel aquifer (ALHOGARATY).

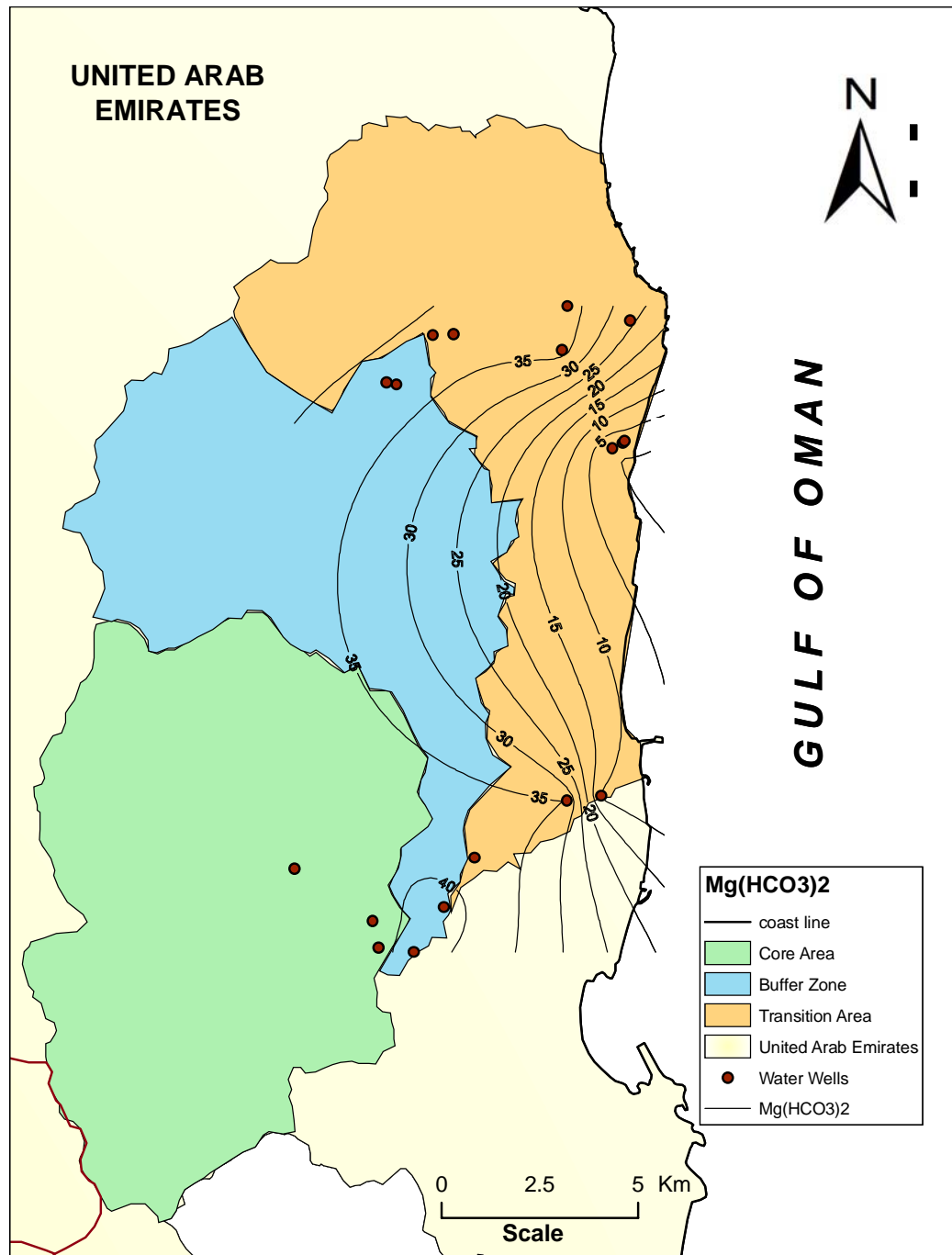


Figure 9.27 Dominance of the $\text{Mg}(\text{HCO}_3)_2$ groundwater dissolved salt (%) in the eastern gravel aquifer (ALHOGARATY).

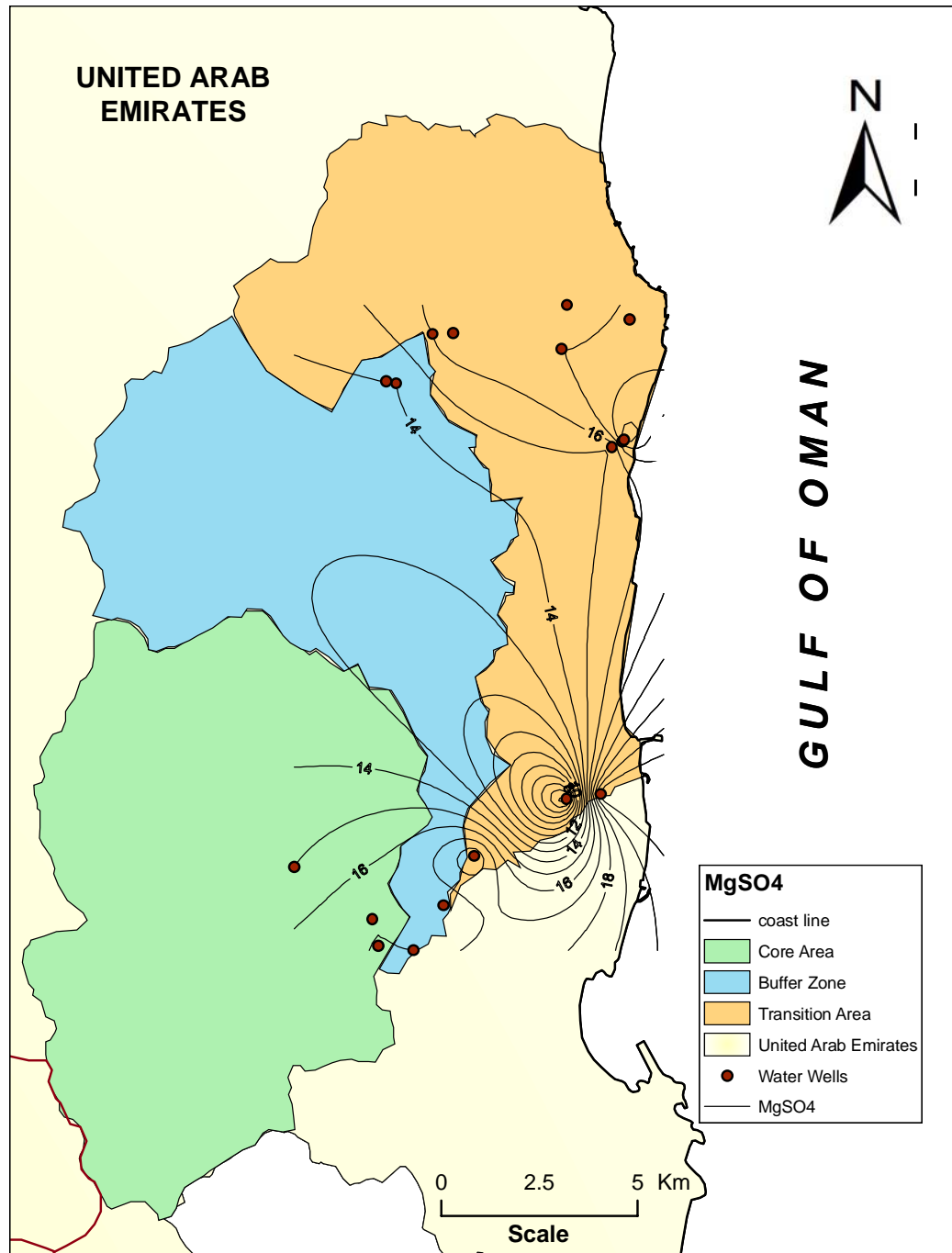


Figure 9.28 Dominance of the MgSO_4 groundwater dissolved salt (%) in the eastern gravel aquifer (ALHOGARATY).

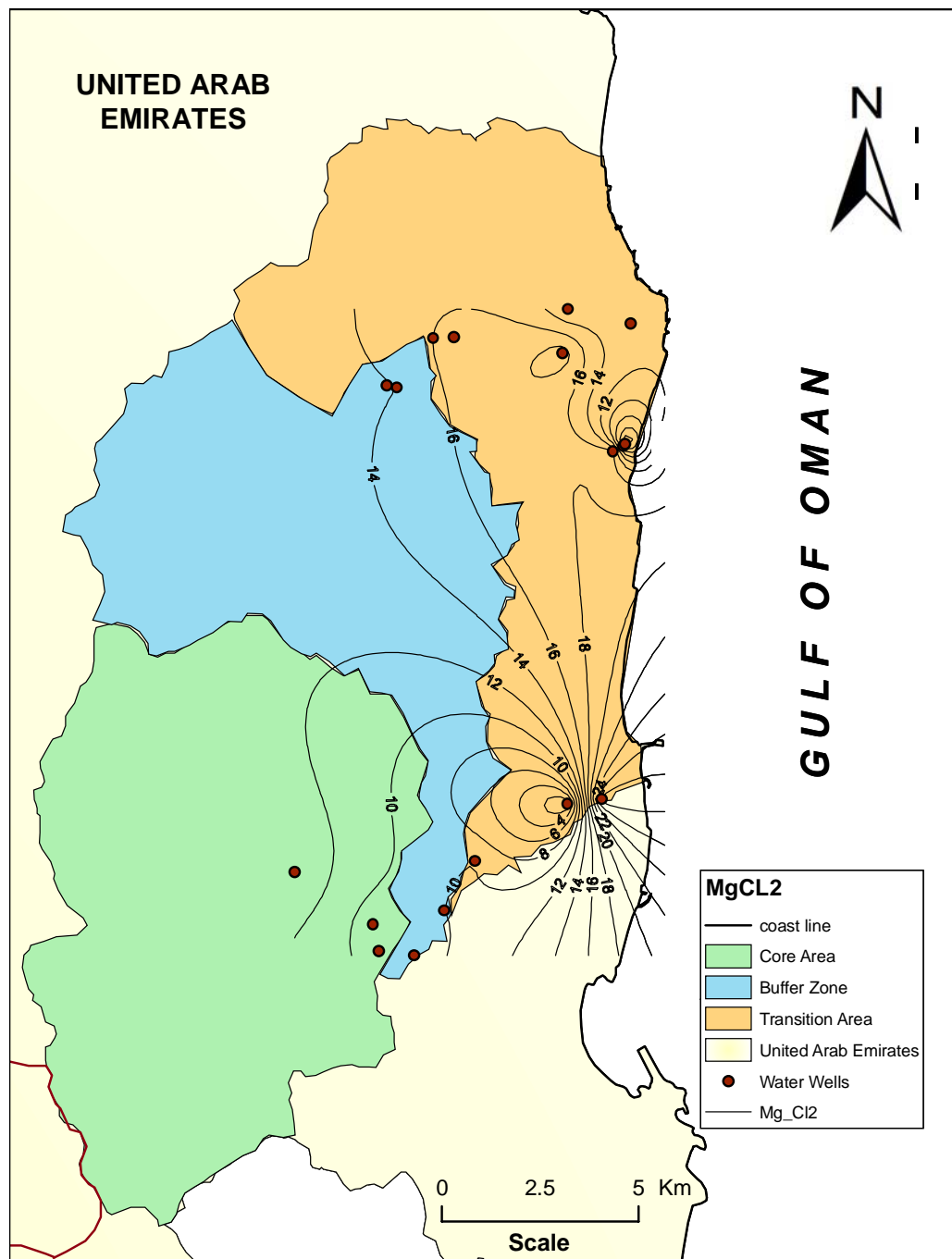


Figure 9.29 Dominance of the $MgCl_2$ groundwater dissolved salt (%) in the eastern gravel aquifer (ALHOGARATY).

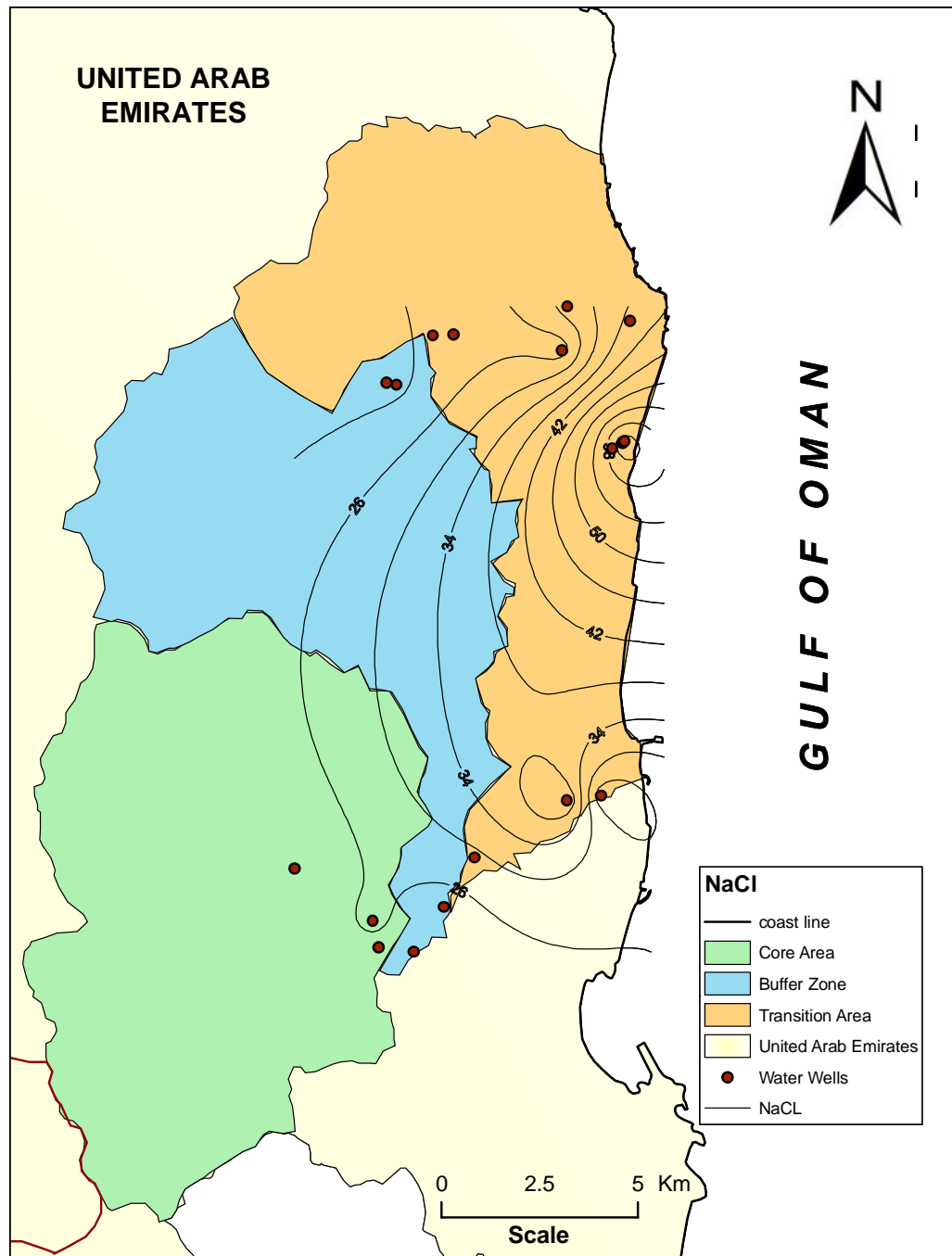


Figure 9.30 Dominance of the NaCl groundwater dissolved salt (%) in the eastern gravel aquifer (ALHOGARATY).

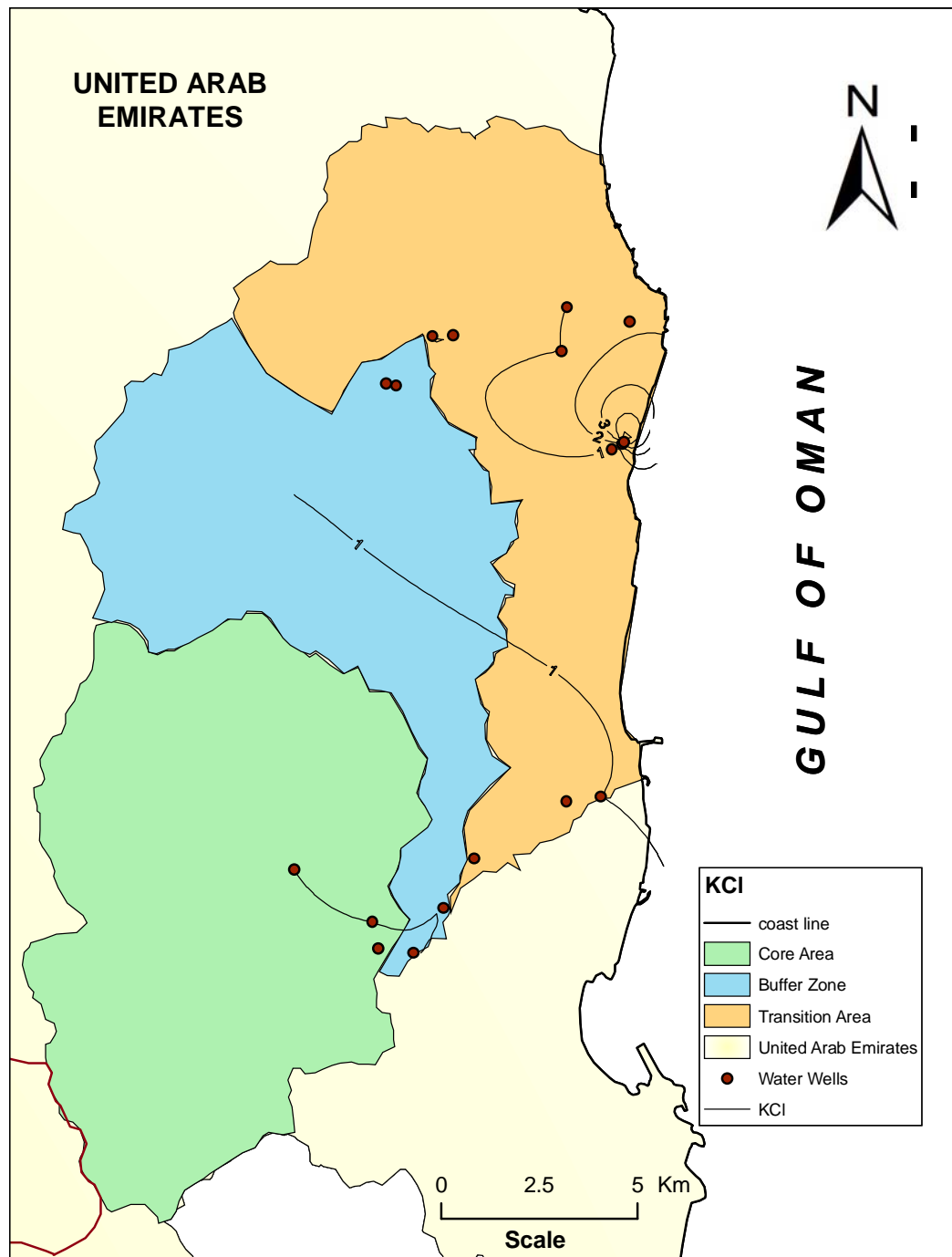


Figure 9.31 Dominance of the KCl groundwater dissolved salt (%) in the eastern gravel aquifer (ALHOGARATY).

9.3.6 Hydrochemical Ratios

Absolute concentrations are commonly used to investigate specific water types. However, because the groundwater in the study area subject to dilution by rainwater or mixing with other water types, the use of absolute concentrations becomes less important. Ion ratios show the relative concentrations of various ions and can be used to indicate the predominance of a particular ion and define locations of salt water intrusion (Ball et al., 1987). The hydrochemical ratios were calculated for the groundwater samples collected from the study area (Table 9.9). These ratios were used to identify the source of groundwater, identify active geochemical reactions and assess the salt water intrusion problem.

Table 9.9 Calculated main hydrochemical ratios for groundwater in the Eastern Coast Region of the UAE in 2009 (ALHOGARATY).

No.	Easting	Northing	Ca/Mg	Na/(Na+Cl)	Na/Cl	Cl/(CO ₃ +HCO ₃)
1	435578	2820142	0.24	0.47	1.11	0.91
2	435616	2820195	0.21	0.48	1.10	0.90
3	436630	2820161	0.26	0.43	1.30	0.95
4	435309	2820013	0.28	0.44	1.30	0.95
5	427193	2809291	0.12	0.30	2.33	0.44
6	429201	2807961	0.14	0.37	1.69	0.43
7	430235	2807161	0.14	0.36	1.82	0.38
8	431007	2808298	0.11	0.35	1.89	0.41
9	431798	2809560	0.06	0.34	1.96	0.50
10	434154	2811024	0.14	0.47	1.12	0.52
11	435021	2811140	0.25	0.24	3.13	0.68
12	429811	2821628	0.20	0.32	2.13	0.40
13	430736	2822891	0.08	0.29	2.44	0.48
14	434025	2822517	0.04	0.31	2.17	0.53
15	431261	2822918	0.06	0.30	2.33	0.50
16	434166	2823637	0.04	0.34	1.96	0.54

The chloride-bicarbonate ratio was recommended as a criterion to evaluate seawater intrusion (for practical purposes, $\text{Cl}^-/(\text{HCO}_3^- + \text{CO}_3^{2-})$ is employed). This ratio is used since chloride is the most dominant anion of ocean water and normally occurs in small amounts in groundwater. On the other hand, bicarbonate is usually the most abundant anion in groundwater and occurs in only minor amount in seawater (Todd, 1980). In the study area, the molar ratio varies between 0.40 and 0.95, with an average

of 0.60 (Table 9.9). The iso $\text{Cl}^-/(\text{HCO}_3^- + \text{CO}_3^{2-})$ ratio contour map shows that the study area in general is not suffering salt water intrusion in the present time (Figure 9.32).

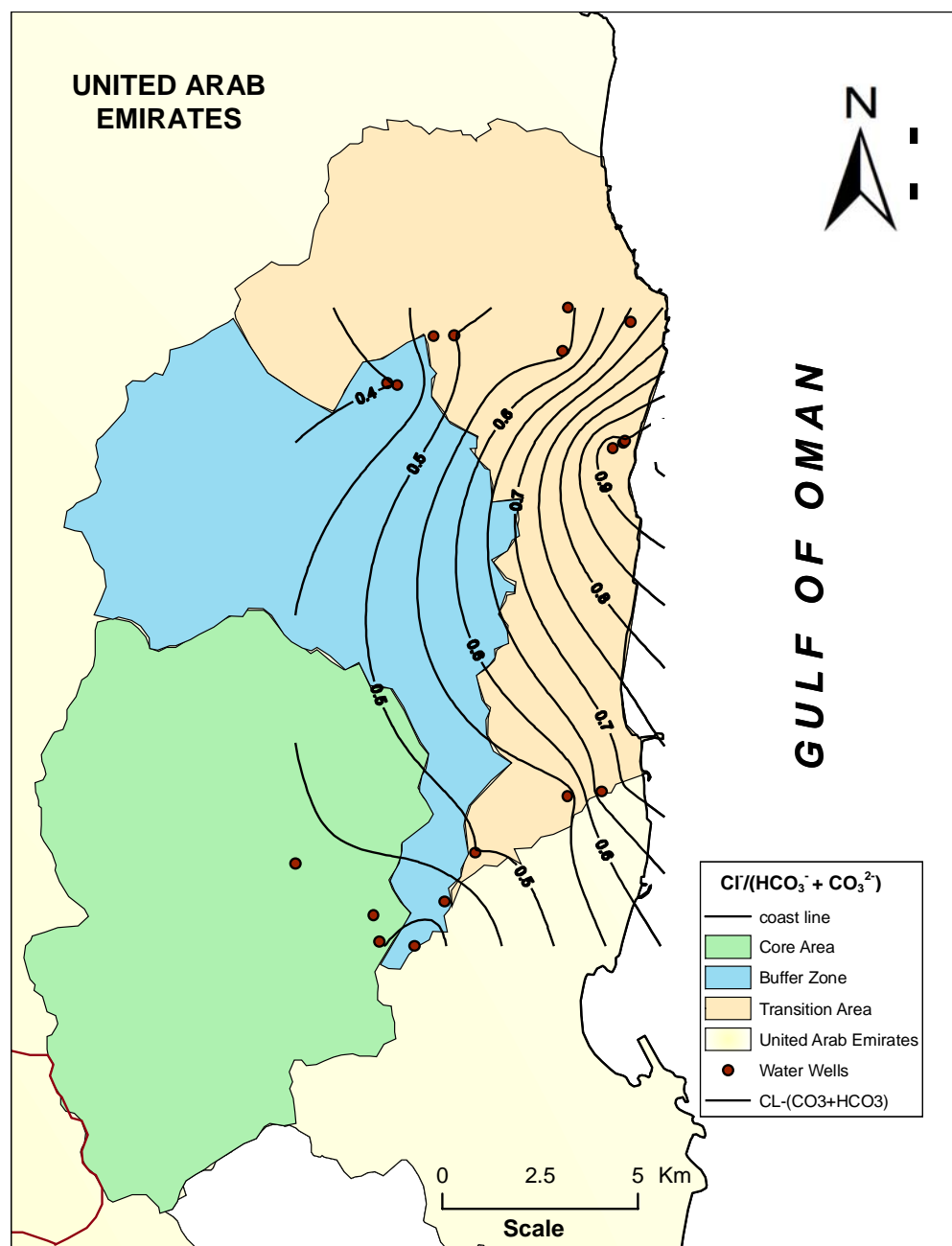


Figure 9.32 Contour map of iso $\text{Cl}^-/(\text{HCO}_3^- + \text{CO}_3^{2-})$ ratio in groundwater within the study area (ALHOGARATY).

However, the groundwater in Dadinah well field is susceptible for salt water intrusion as $\text{Cl}^-/(\text{HCO}_3^- + \text{CO}_3^{2-})$ ratio in this area is approaching 1 and may exceed it 1.0 (between 0.91 and 0.95; Table 9.9). The Na/Cl ratio is also used to indicate areas suffering from salt water intrusion. The ratio in sea water is less than unity (0.85), while groundwater has ratios greater than 1.0 (Table 9.10) (Hounslow, 1995). The Na/Cl is greater than 1.0 in all sampled water wells (Figure 9.33).

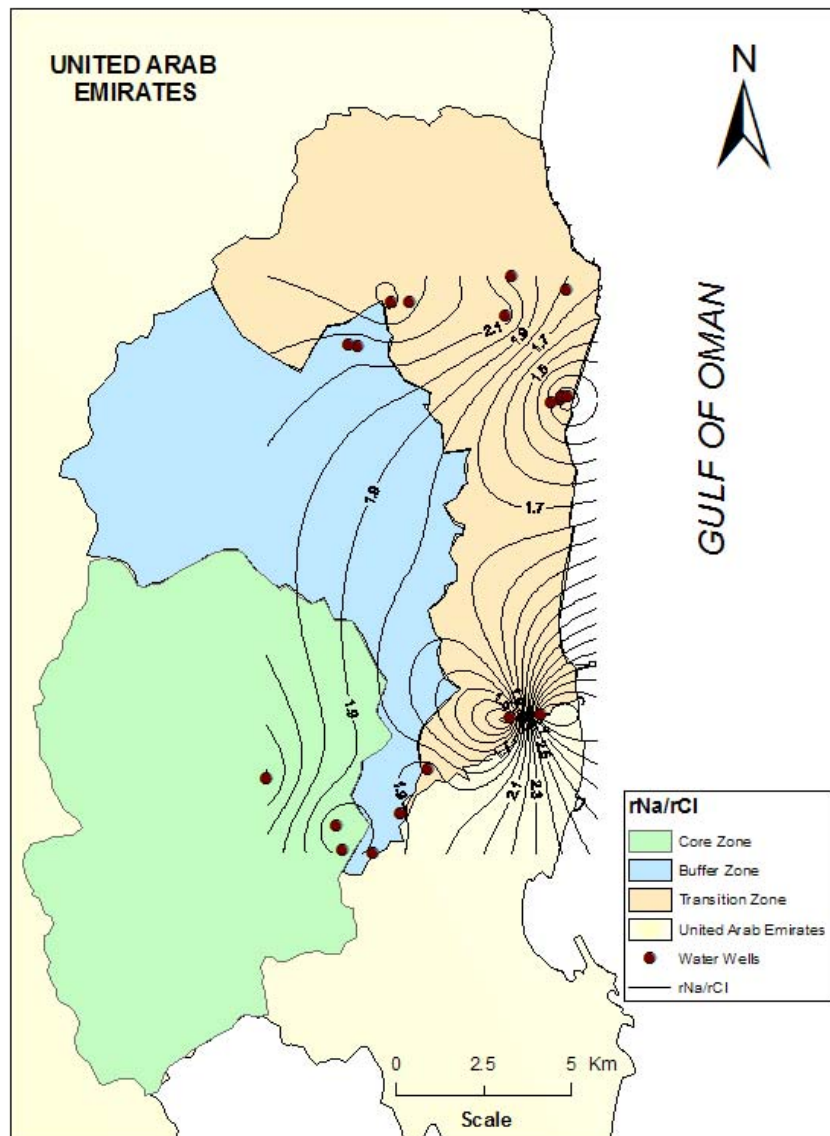


Figure 9.33 Contour map of iso (Na^+/Cl^-) ratio in groundwater within the study area (ALHOGARATY).

The $\text{Na}^+ / (\text{Na}^+ + \text{Cl}^-)$ ratio > 0.5 and TDS < 500 mg/l suggest reverse softening or saline intrusion (Hounslow, 1998). In the study area, the ratio is mainly < 0.5 , while the TDS is < 500 mg/l, which may not indicate salt water intrusion. But, water-rock interaction and ion exchange can an active process in such dynamic area (Figure 9.34).

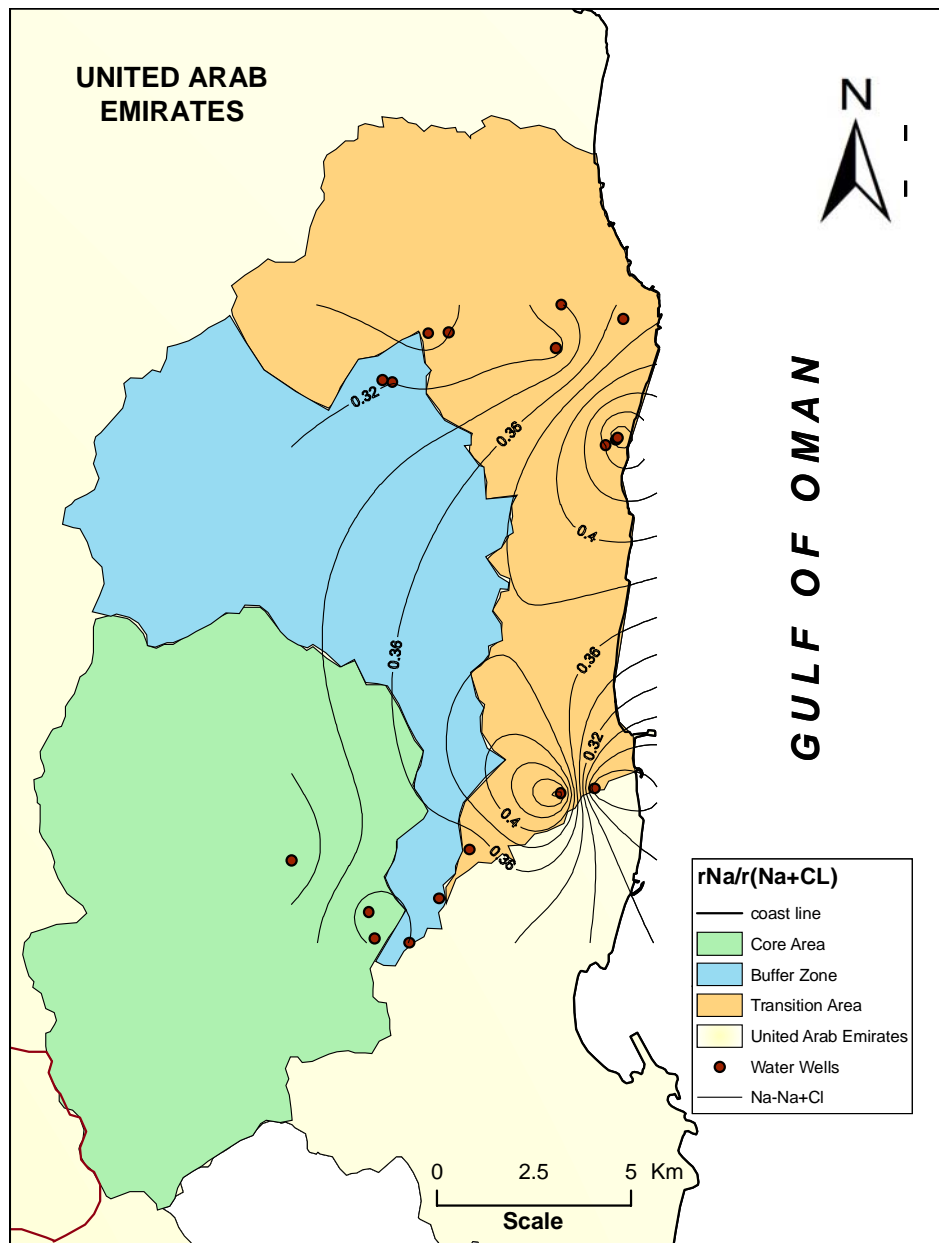


Figure 9.34 Contour map of iso $\text{Na}^+ / (\text{Na}^+ + \text{Cl}^-)$ ratio in groundwater within the study area (ALHOGARATY).

The low $\text{Ca}^{2+}/\text{Mg}^{2+}$ (0.19) may indicate salt water intrusion. But, because the study area is dominated by Ophiolite and gravels of Ophiolitic origin, the small ($\text{Ca}^{2+}/\text{Mg}^{2+}$) ratio is basically related to Ophiolite weathering (Figure 9.35).

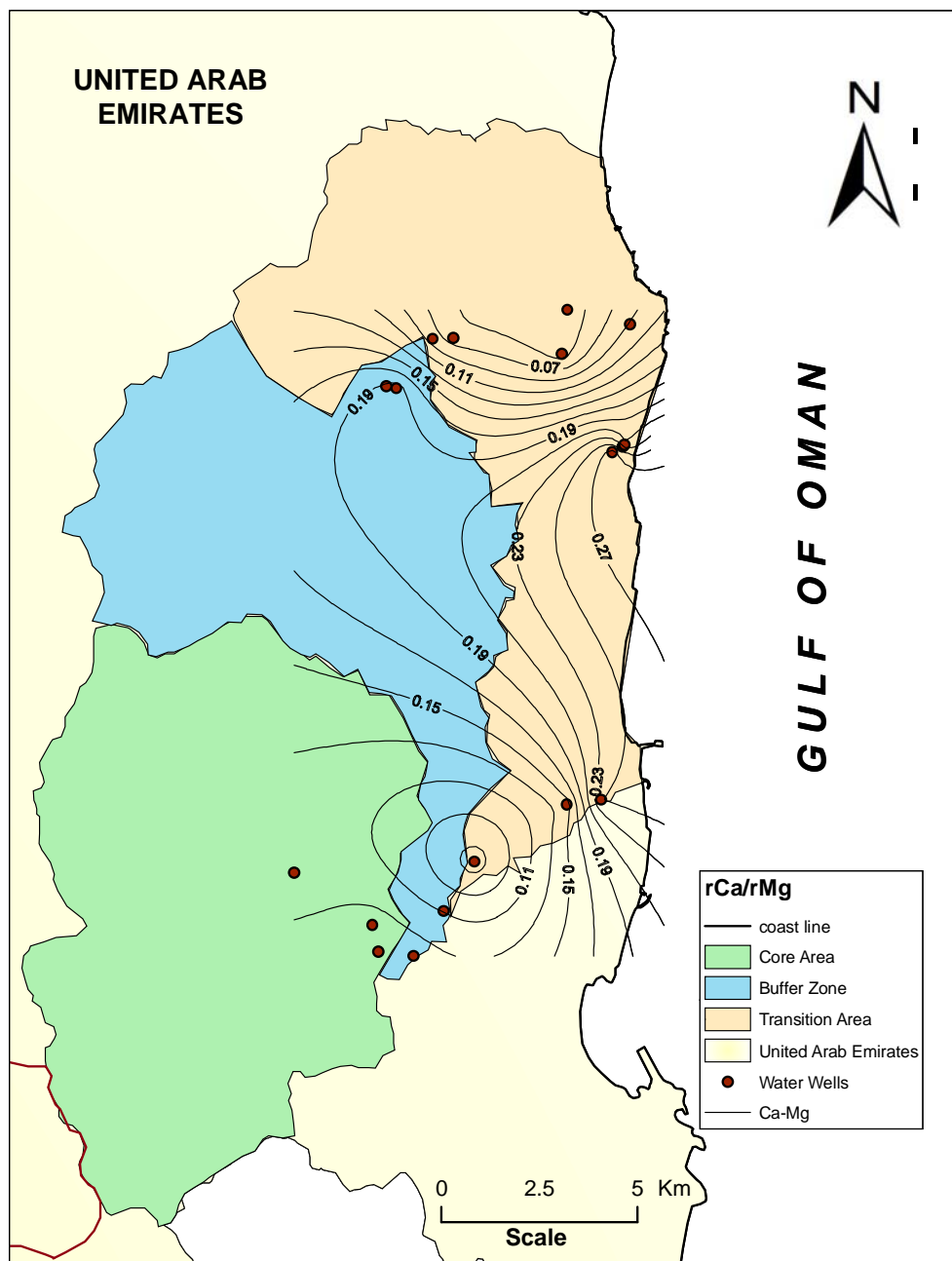


Figure 9.35 Contour map of iso ($\text{Ca}^{2+}/\text{Mg}^{2+}$) ratio in groundwater within the study area (ALHOGARATY).

Table 9.10 showing the use of hydrochemical ratios used for identification of the possible sources of groundwater in the study area (ALHOGARATY).

Ratio	Suggested value (Hounslow, 1995)	Indication	Ratio in the study area (Table 9.9)
$\text{Cl}^-/(\text{HCO}_3^- + \text{CO}_3^{2-})$	<1 >1	Fresh water dominant Saline dominant	0.40-0.95
Na^+/Cl^-	<0.85 >1	Saline dominant Fresh water dominant	1.10-3.13
$\text{Na}^+/(\text{Na}^+ + \text{Cl}^-)$	>0.5, TDS>500	Ionic exchange	0.29-0.48
$\text{Ca}^{2+}/\text{Mg}^{2+}$	<0.5	Ophiolite weathering	0.04-0.28

9.3.7 Trilinear Diagram

The main purpose of the trilinear diagram proposed by Piper (1944) is to identify different water types in a particular area. The diamond-shaped field of this diagram consists of two equal triangular fields. Generally, water which appears in the upper triangle has secondary salinity properties, where $(\text{SO}_4^{2-} + \text{Cl}^-)$ exceed $(\text{Na}^+ + \text{K}^+)$ and the characteristic water types are Ca and Mg chlorides and sulphates. On the other hand, water appearing in the lower triangle are considered to have primary alkalinity properties where $(\text{CO}_3^{2-} + \text{HCO}_3^-)$ exceed $(\text{Ca}^{2+} + \text{Mg}^{2+})$, and the characteristic water types are Na and K carbonates and bicarbonates (Walton, 1970). Figure 9.36 shows a trilinear plot of major ions in groundwater samples collected from the study area. Because most samples appear in the upper triangle of the diamond-shaped field, the dominant groundwater types are Ca and Mg chlorides and sulphates. Groundwater in the study area is highly enriched in Mg^{2+} , which dissolve from the ultramafic ophiolitic rocks dominating the study area. Based on the calculated water dissolved salts and the trilinear plot, the groundwater types dominating the study area are: $\text{Ca}(\text{HCO}_3)_2$ and $\text{Mg}(\text{HCO}_3)_2$ water type in the north and south, and NaCl water type is dominant in Dadinah area, where heavy groundwater pumping for all purposes is taking place.

9.4 Groundwater Evaluation

Water quality determines its suitability for domestic and agricultural purposes. The suitability of groundwater for a particular purpose depends on specific quality criteria

defined by international and regional organizations. Quality limits of water supplies for drinking, irrigation and industrial uses apply to groundwater because of its extensive development for these purposes (Todd, 1980).

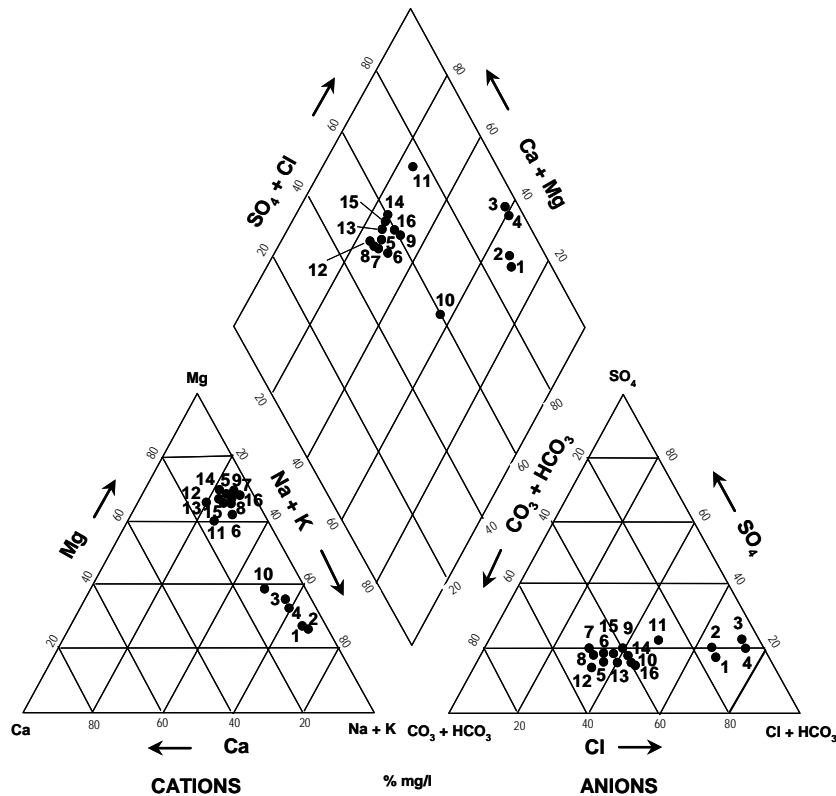


Figure 9.36 Presentation of groundwater chemistry in the study area on the trilinear diagram (ALHOGARATY).

9.4.1 Domestic Purposes

Usually, water applied for domestic purposes has certain standard specifications as regards to its physical, chemical, biological and radioactive properties. These standards are intended primarily to protect human health. The World Health Organization (WHO, 1985) sets these standards and the food control laboratories in different UAE municipalities monitor their implementation. According to the TDS content, groundwater in the study area can be divided into an eastern fresh water

region (TDS < 1,000 mg/l), a central brackish water region (TDS between 1,000 and 10,000 mg/l) and a western saline water region (TDS > 10,000 mg/l) (Figure 9.36; Table 9.7). Total water hardness is defined as the sum of Ca^{2+} and Mg^{2+} concentrations expressed as mg/l of CaCO_3 (Bouwer, 1978). Water is classified according its hardness into soft water (< 60 mg/l), moderately hard water (61-120 mg/l), hard water (121-180 mg/l) and very hard water (> 180 mg/l) (Hem, 1970).

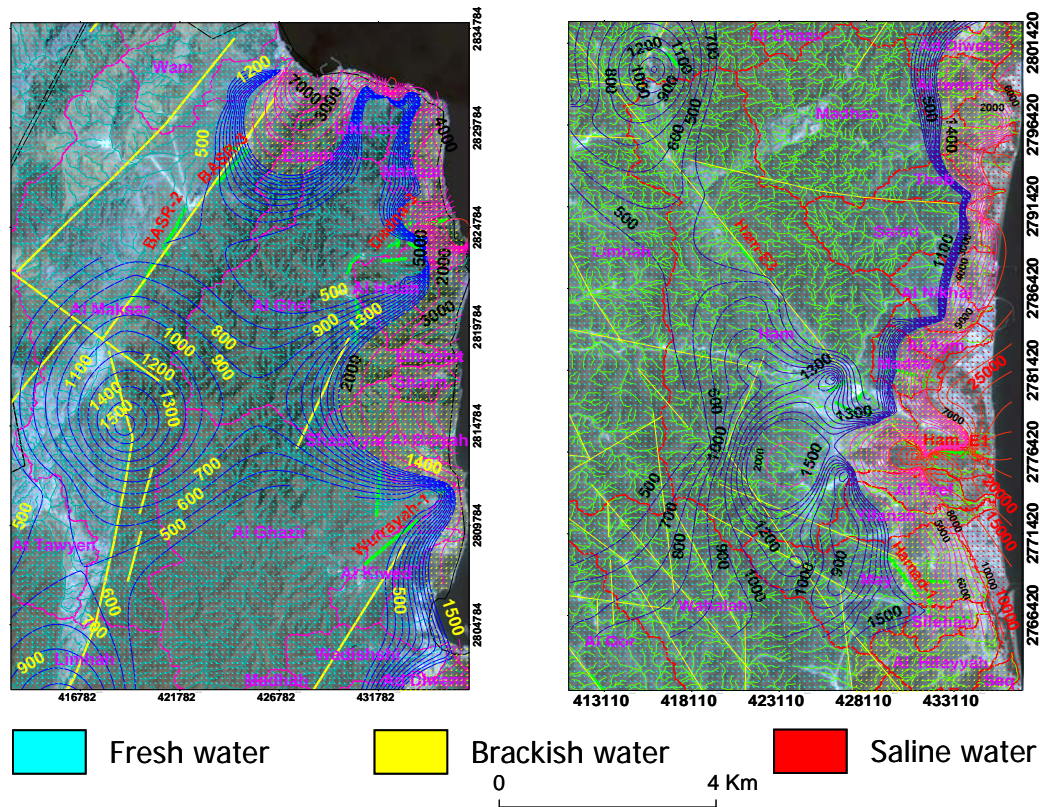


Figure 9.37 Groundwater types in the study area based on the concentration of total dissolved solids (TDS) (modified after Almatari, 2010).

Except for the western part, most of groundwater in the study area is hard to very hard (Figures 9.38 and 9.39). Groundwater hardness increased slightly between 2005 and 2009 sampling period (Tables 9.5 and 9.6), possibly due to excessive groundwater pumping for all purposes.

9.4.2 Agricultural Purposes

For evaluation the suitability of groundwater in the study area for agricultural uses, the effect of water on plants and soils is assessed. The sodium ion concentration is important in classifying irrigation water because sodium reacts with soil and reduces its permeability. The Sodium Adsorption Ratio (SAR) is defined by the following equation:

$$SAR = \frac{Na}{\sqrt{(Ca + Mg) / 2}}$$

This equation is used for evaluating the suitability of water for irrigation purposes. Concentrations of Na^+ , Mg^{2+} and Ca^{2+} are expressed in milliequivalent per liter (meq/L). According to the SAR values (Figures 9.40 and 9.41), groundwater in most of the study area has a limited harmful effect on plants when used for irrigation.

In the central part of the study area ground water can cause moderate to high harmful effects for plants when applied for irrigation. In the west central and southeastern parts of the study area, groundwater can have moderate to high harmful effects if used for irrigation of traditional crops. Figure 9.42 was constructed by the U. S. Salinity Laboratory Staff for evaluation the suitability of water for irrigation purposes. According to this graph, water lies in three zones the lower left zone (Green) is characterized by low salinity and low SAR, and is suitable for irrigating almost all crops. The middle zone (Blue) has fair quality water and can be used for irrigation a large number of crops. The right, upper zone (yellow) is characterized by high salinity and high SAR values and considered hazardous for irrigation purposes.

Based on the measured EC and calculated SAR values for water samples from the eastern gravel aquifer, most groundwater in the eastern gravel aquifer is good for irrigation purposes. A few groundwater samples (in the yellow zone) are not suitable for irrigating traditional crops and can cause harmful to plants and soils when used for irrigation.

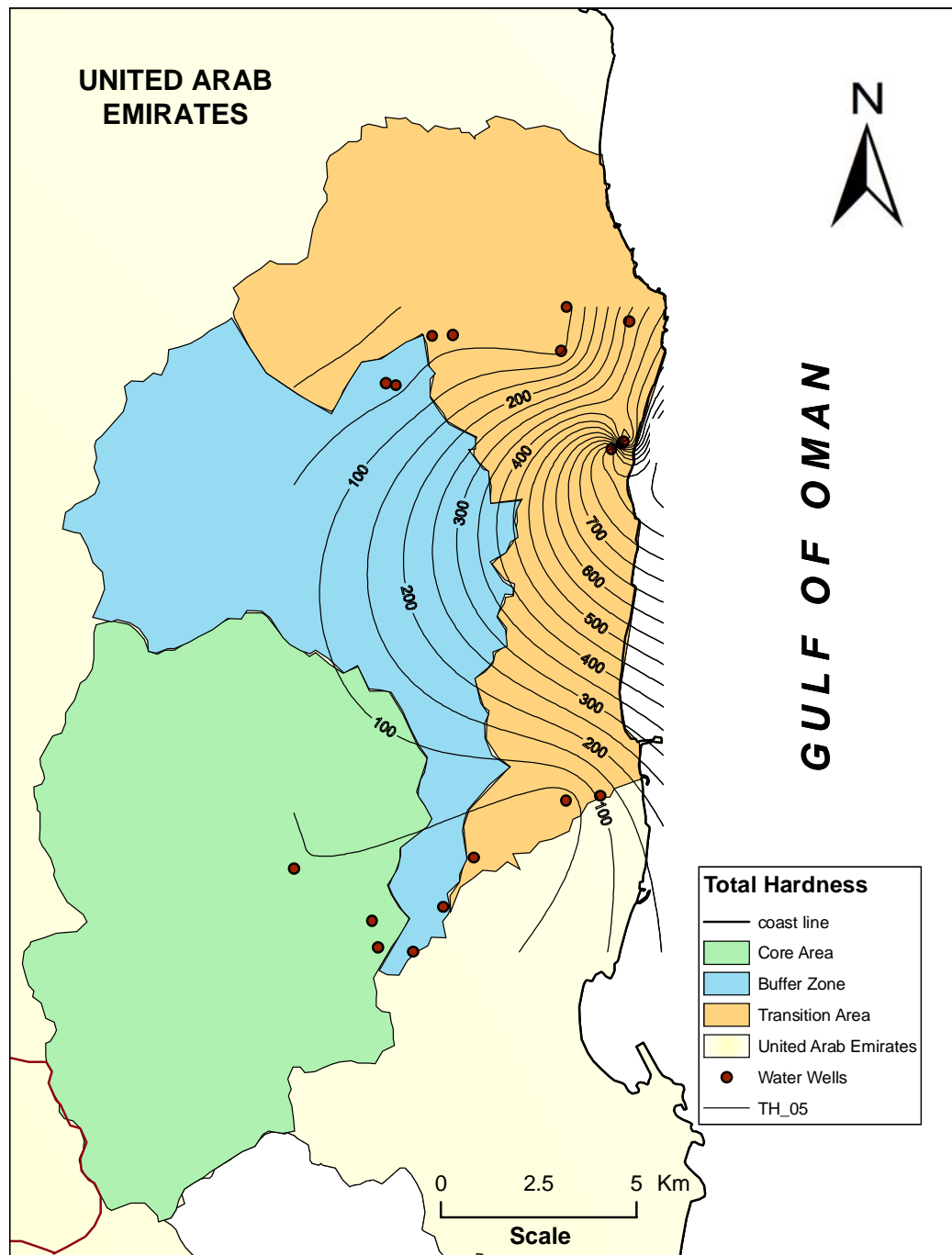


Figure 9.38 Total hardness (TH in mg/l) of groundwater samples collected from the study area in 2005 (ALHOGARATY).

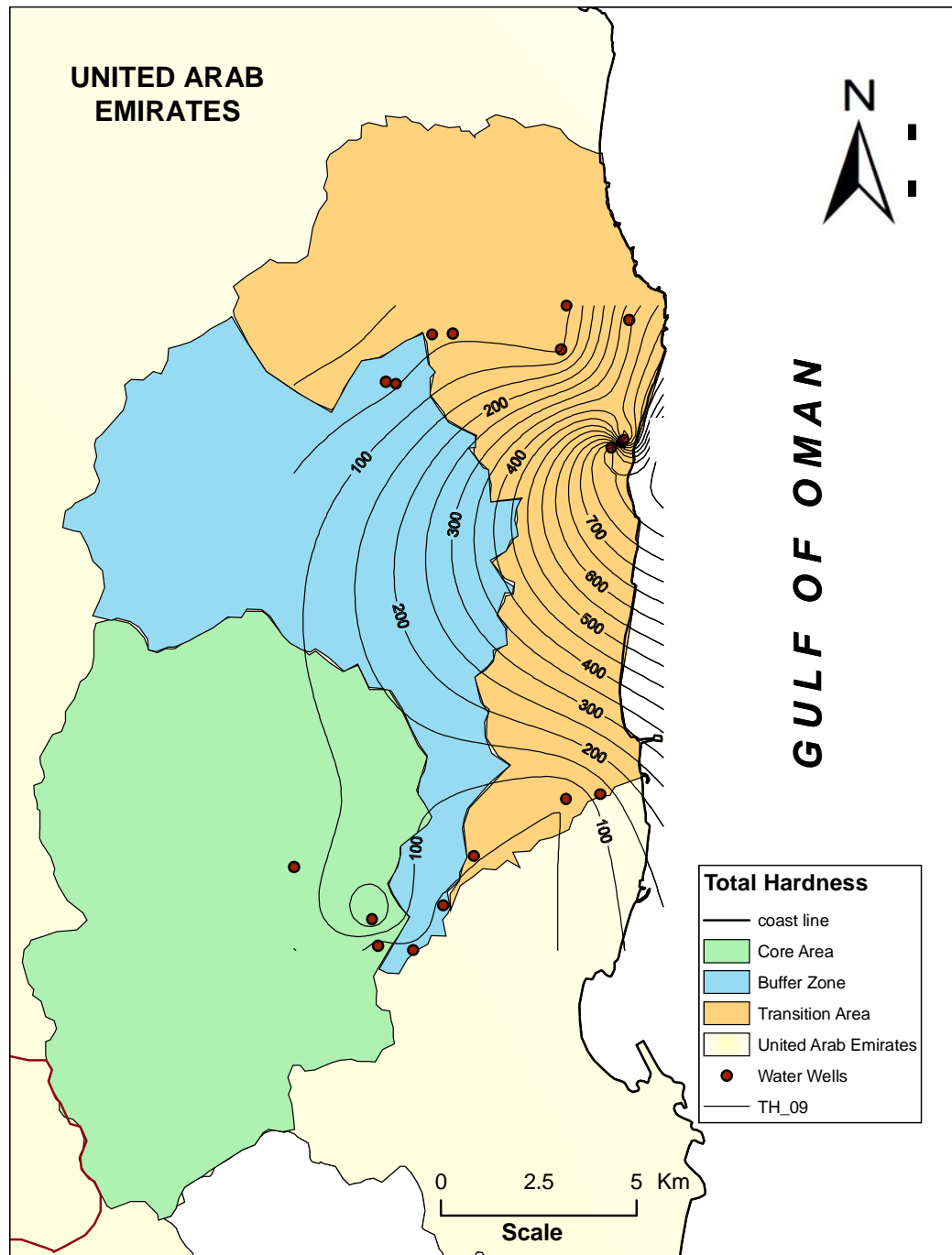


Figure 9.39 Total hardness (TH in mg/l) of groundwater samples collected from the study area in 2009 (ALHOGARATY).

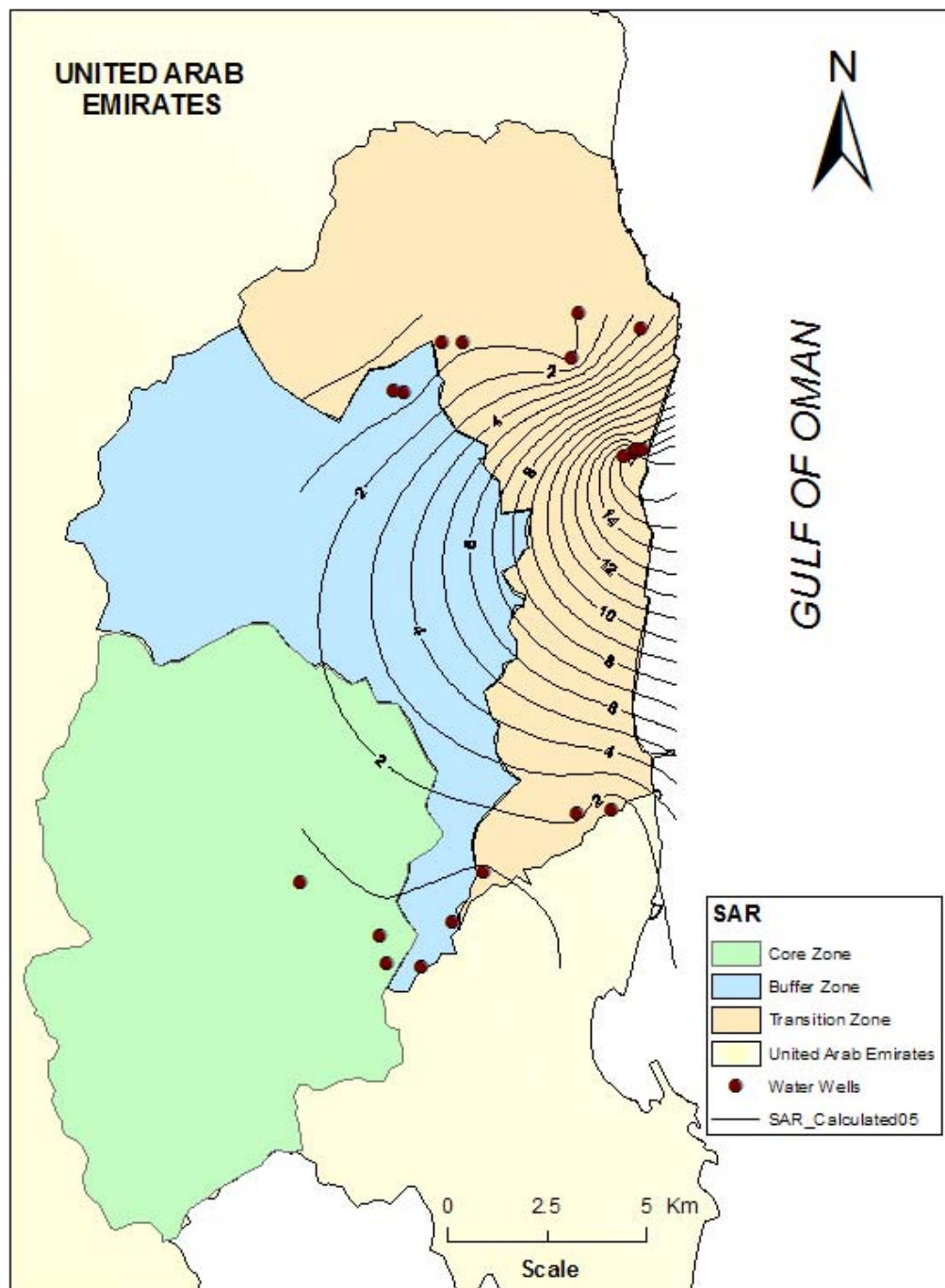


Figure 9.40 Sodium adsorption ratios (SAR) of groundwater samples collected from the study area in 2005 (ALHOGARATY).

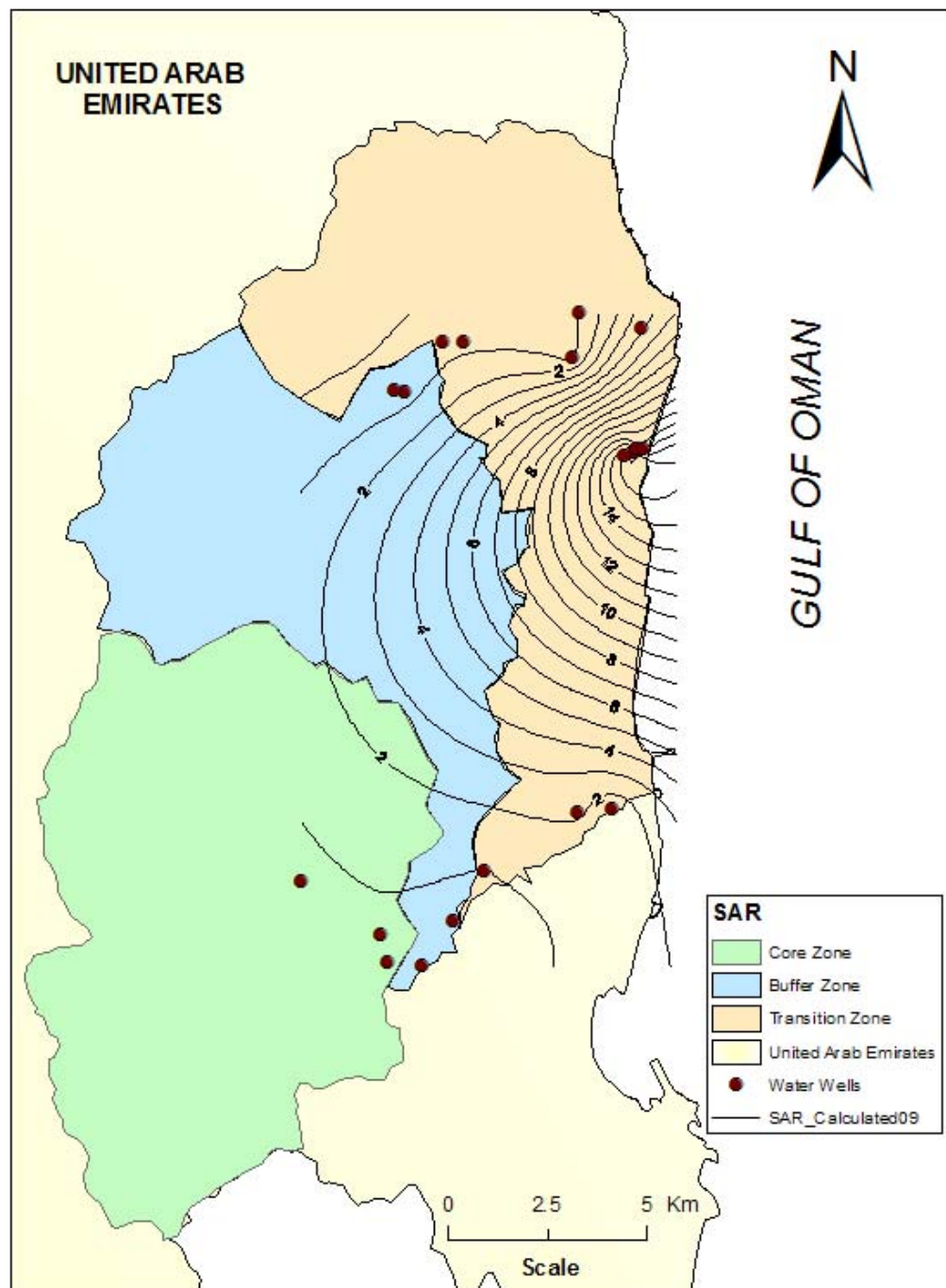


Figure 9.41 Sodium adsorption ratios (SAR) of groundwater samples collected from the study area in 2009 (ALHOGARATY).

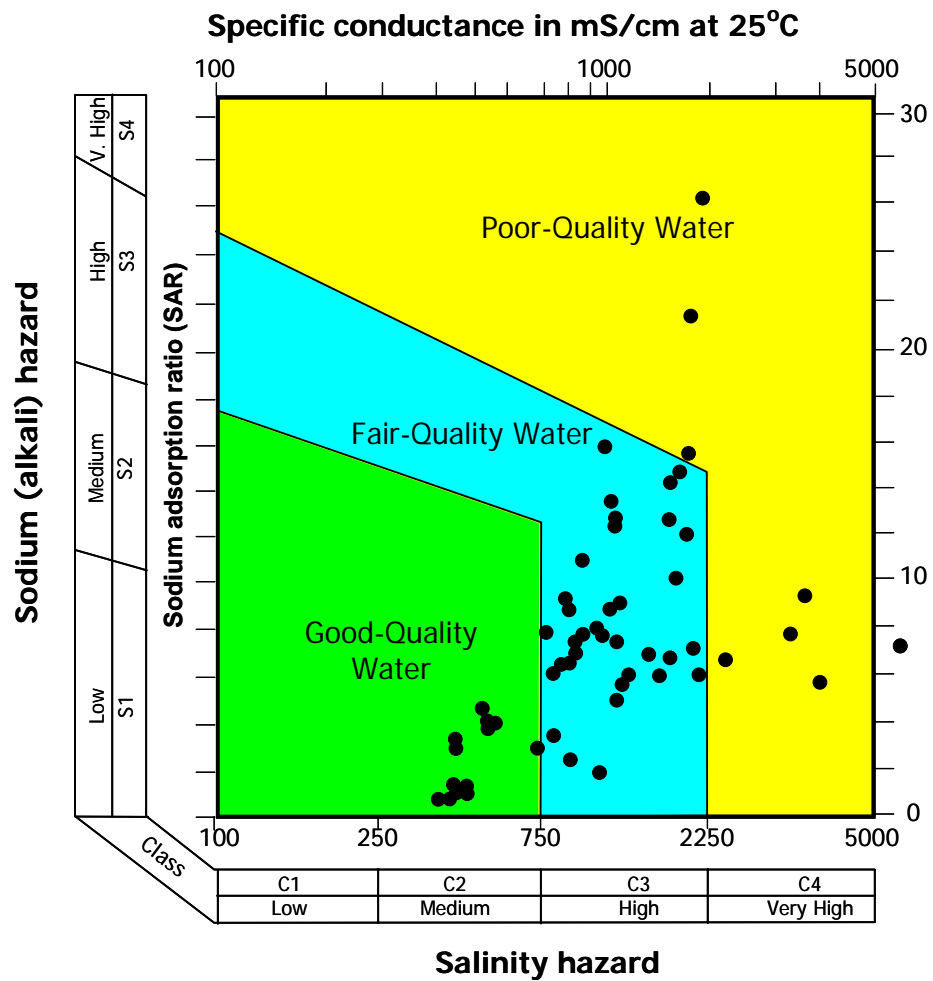


Figure 9.42 Evaluation of the suitability of groundwater in the eastern gravel aquifer in the UAE for irrigation (Rizk and Alsharhan, 2008).